

A continuum of periodic solutions to the planar four-body problem with various choices of masses

Tiancheng Ouyang

Department of Mathematics, Brigham Young University
Provo, Utah 84602, USA

Email: ouyang@math.byu.edu

Zhifu Xie

Department of Mathematics and Computer Science
Virginia State University

Petersburg, Virginia 23806, USA

Email: zxie@vsu.edu

Abstract

In this paper, we apply the variational method with the Structural Prescribed Boundary Conditions (SPBC) to prove the existence of periodic and quasi-periodic solutions for planar four-body problem with $m_1 = m_3$ and $m_2 = m_4$. A path $q(t)$ in $[0, T]$ satisfies SPBC if the boundaries $q(0) \in \mathbf{A}$ and $q(T) \in \mathbf{B}$, where \mathbf{A} and \mathbf{B} are two structural configuration spaces in $(\mathbf{R}^2)^4$ and they depend on a rotation angle $\theta \in (0, 2\pi)$ and the mass ratio $\mu = \frac{m_2}{m_1} \in \mathbf{R}^+$.

We show that there is a region $\Omega \subseteq (0, 2\pi) \times \mathbf{R}^+$ such that there exists at least one local minimizer of the Lagrangian action functional on the path space satisfying SPBC $\{q(t) \in H^1([0, T], (\mathbf{R}^2)^4) \mid q(0) \in \mathbf{A}, q(T) \in \mathbf{B}\}$ for any $(\theta, \mu) \in \Omega$. The corresponding minimizing path of the minimizer can be extended to a non-homographic periodic solution if θ is commensurable with π or a quasi-periodic solution if θ is not commensurable with π . In the variational method with SPBC, we only impose constraints on boundary and we do not impose any symmetry constraint on solutions. Instead, we prove that our solutions extended from the initial minimizing pathes have the symmetries.

The periodic solutions can be further classified as simple choreographic solutions, double choreographic solutions and non-choreographic solutions. Among the many stable simple choreographic orbits, the most extraordinary one is the stable star pentagon choreographic solution when $(\theta, \mu) = (\frac{4\pi}{5}, 1)$. Remarkably the unequal-mass variants of the stable star pentagon are just as stable as the basic equal mass choreography (See figure 1).

Key word: Variational Method, Choreographic Periodic Solutions, Structural Prescribed Boundary Conditions (SPBC), Stability, Central Configurations, n -body Problem.

AMS classification number: 37N05, 70F10, 70F15, 37N30, 70H05, 70F17

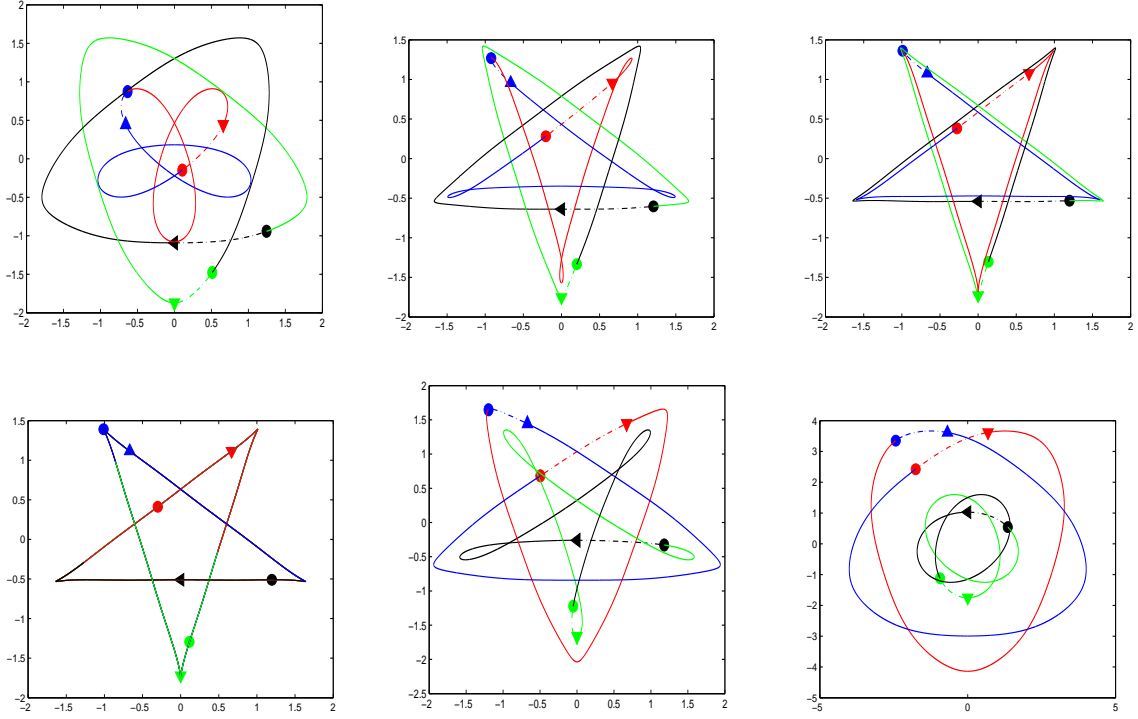


Figure 1: $\theta = \frac{4\pi}{5}$, $m_1 = m_3 = 1, m_2 = m_4 = \mu$. From left to right $\mu = 0.3, 0.8, 0.95, 1, 1.5$, and 10 . Solutions start from an isosceles triangle $q(0)$ (circular spots) with one in the axis of its symmetry to another isosceles triangle $q(T)$ (triangular spots).

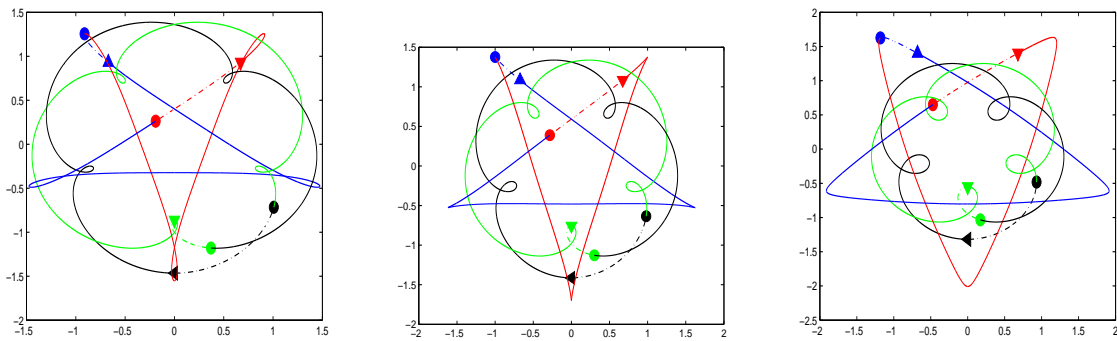


Figure 2: $\theta = \frac{4\pi}{5}$, $m_1 = m_3 = 1, m_2 = m_4 = \mu$. From left to right $\mu = 0.8, 1$, and 1.5 . Solutions start from an isosceles triangle $q(0)$ (circular spots) with one in the axis of its symmetry to another isosceles triangle $q(T)$ (triangular spots).

1 Introduction

Given n bodies, let m_i denote the mass and $q_i(t)$ denote the position in \mathbf{R}^d , $d \geq 2$ of body i at time t in d -dimensional space. The *action functional* is a mapping from the space of all trajectories $q_1(t), q_2(t), \dots, q_n(t)$ into the reals. It is defined as the integral:

$$(1) \quad \mathcal{A}(q(t)) = \int_0^T K(\dot{q}(t)) + U(q(t)) dt,$$

where $K(\dot{q}(t)) = \frac{1}{2} \sum_{i=1}^n m_i |\dot{q}_i(t)|^2$ is the kinetic energy and U is the Newtonian potential function $U = \sum_{1 \leq i < j \leq n} \frac{m_i m_j}{|q_i - q_j|}$. Critical points of the action functional are trajectories that satisfy the equations of motion, i.e. Newton's equations:

$$(2) \quad m_i \ddot{q}_i = \frac{\partial U}{\partial q_i} = \sum_{j=1, j \neq i}^n \frac{m_i m_j (q_j - q_i)}{|q_j - q_i|^3} \quad 1 \leq i \leq n.$$

Without loss of generality, we assume that the center of mass $c = (1/M) \sum_{i=1}^n m_i q_i$ is always at the origin, where $M = \sum m_i$ is the total mass. Let $p_i = m_i \dot{q}_i$. Then the Hamiltonian of the Newton's equations is

$$(3) \quad H(q, p) = \sum_{i=1}^n \frac{|p_i|^2}{2m_i} - U(q).$$

In the past decade, the existence of many new interesting periodic orbits are proved by using variational method for the n-body problem. Most of them are found by minimizing the Lagrangian action on a symmetric loop space with some topological constraints (for example, see [3, 4, 11, 15, 16, 17, 33, 34]).

Following the notions in [3, 9], a *simple choreographic solution* (for short, choreographic solution) is a periodic solution that all bodies chase one another along a single closed orbit. If the orbit of a periodic solution consists of two closed curves, then it is called a *double-choreographic solution*. If the orbit of a periodic solution consists of three closed curves, then it is called a *triple-choreographic solution*. If the orbit of a periodic solution consists of different closed curves, each of which is the trajectory of exact one body, it is called *non-choreographic solution*. Many relative equilibria give rise to simple choreographic solutions and they are called trivial choreographic solutions (circular motions). After the discovery of the first remarkable non-trivial choreographic solution – the figure eight of the three body problem by Moore (1993 [24]) and Chenciner and Montgomery (2000, [8]), many expertise attempt to study choreographic solutions and a large number of simple choreographic solutions have been discovered numerically but very few of them have rigorous existence proofs. More results can be found in [2, 5, 6, 9, 10, 12, 14, 15] and the reference therein.

In this paper, we are interested in the action minimizing solutions in path space satisfying the SPBC for planar four-body problem with unequal masses. We prove the existence of periodic and quasi-periodic orbits for two pairs of unequal masses. We look for the continuum of the periodic and quasi-periodic solutions for equal masses discovered by the variational method

with SPBC developed in the recent paper [26]. Among the many stable simple choreographic orbits in [26], the most extraordinary one is the stable star pentagon choreographic solution. The variants of star pentagon from equal mass to unequal mass is continuously deforming from simple choreographic orbit to double choreographic orbits (see figure 1).

Figure eight is a remarkably non-trivial simple choreographic solution, but more importantly, it is stable and the stability was proved in ([19, 25]). It seems very hard to find a stable simple choreographic solution (C. Simó [30] and R. Vanderbei [35]). To the best knowledge of the authors, all of the above known simple choreographic solutions are unstable except the figure eight [8, 24] and the family of star pentagon [26]. The journal *Science* had two articles [21, 28] on the figure-eight orbit. They deal with the idea that there could exist a planet system of equal masses. But the window of stability of figure-eight orbit is very small with slightly change of masses. Hence it seems unlikely that any real stars follow such an orbit. Significantly different from the remarkable figure-eight orbit, the unequal-mass variants of the stable star pentagon seem to be just as stable as the basic equal mass choreography. This fact makes the beautiful star pentagon orbit all the more remarkable because such periodic solutions actually have more chance to be seen in some quadruple star system.

In order to get a possible preassigned periodic orbit, we have to find an appropriate SPBC. Throughout the paper, we assume $m_1 = m_3$ and $m_2 = m_4$ and let $\mu = \frac{m_2}{m_1}$. Let $\Gamma = \mathbf{R}^6$ and the rotation matrix $R(\theta) = \begin{pmatrix} \cos(\theta) & -\sin(\theta) \\ \sin(\theta) & \cos(\theta) \end{pmatrix}$.

Our Settings on SPBC:

Given $\vec{a} = (a_1, a_2, \dots, a_6) \in \Gamma$, two fixed configurations are defined by $Qstart = \begin{pmatrix} 0 & -a_3 \\ -a_1 & a_2 \\ 0 & \frac{-m_2 a_2 - m_4 a_2 + m_1 a_3}{m_3} \\ a_1 & a_2 \end{pmatrix} R(\theta)$, and $Qend = \begin{pmatrix} a_4 & a_5 \\ 0 & -a_6 \\ -a_4 & a_5 \\ 0 & \frac{-m_1 a_5 - m_3 a_5 + m_2 a_6}{m_4} \end{pmatrix}$. Let

$$(4) \quad \mathcal{P}(Qstart, Qend) := \{q(t) \in H^1([0, T], (\mathbf{R}^2)^4) \mid q(0) = Qstart, q(T) = Qend\}.$$

Then the set $S(\vec{a})$ of minimizers is defined by

$$S(\vec{a}) = \{q(t) = (q_1, q_2, q_3, q_4)(t) \in C^2((0, T), (\mathbf{R}^2)^4) \mid q(0) = Qstart, q(T) = Qend, \\ q(t) \text{ is a minimizer of the action functional } \mathcal{A} \text{ over } \mathcal{P}(Qstart, Qend)\}.$$

So the configuration of the bodies changes from an isosceles triangle with one on the axis of symmetry to another isosceles triangle for some positive \vec{a} .

For any given $\vec{a} \in \Gamma$, the minimizers of \mathcal{A} that connect $Qstart$ and $Qend$ are classical collision-free solutions in the interval $(0, T)$. The motion starting from $Qstart$ to $Qend$ will continue beyond the $Qend$ under the universal gravitation but the continuation is hard to predict in general. The second minimizing process can find an appropriate \vec{a} such that the motion can be extended in the way we expected.

The real value function $\tilde{\mathcal{A}}(\vec{a}) : \Gamma \rightarrow \mathbf{R}$ is well defined by

$$(5) \quad \tilde{\mathcal{A}}(\vec{a}) = \int_0^T \frac{1}{2} \sum_{i=1}^n m_i \|\dot{q}_i(t; \vec{a})\|^2 + U(q(t; \vec{a})) dt,$$

where $q(t; \vec{a}) \in S(\vec{a})$ is a minimizer of the action functional \mathcal{A} over $\mathcal{P}(Q_{start}, Q_{end})$ for the given $\vec{a} \in \Gamma$. If it is clear that $q(t; \vec{a})$ is a minimizer for the given \vec{a} from context, we still use $q(t)$ for $q(t; \vec{a})$ for convenience.

Let $\vec{a}_0 = (a_{10}, a_{20}, \dots, a_{60}) \in \Gamma$ be a minimizer of $\tilde{\mathcal{A}}(\vec{a})$ over the space Γ and the corresponding path $q^*(t) = q^*(t; \vec{a}_0) \in S(\vec{a}_0)$, i.e.

$$(6) \quad \begin{aligned} \tilde{\mathcal{A}}(\vec{a}_0) &= \min_{\vec{a} \in \Gamma} \tilde{\mathcal{A}}(\vec{a}) = \min_{\vec{a} \in \Gamma} \left\{ \inf_{q(t) \in \mathcal{P}(Q_{start}, Q_{end})} \mathcal{A}(q(t)) \right\} \\ &= \min_{\vec{a} \in \Gamma} \left\{ \inf_{q(t) \in \mathcal{P}(Q_{start}, Q_{end})} \int_0^T \frac{1}{2} \sum_{i=1}^n m_i \|\dot{q}_i(t)\|^2 + U(q(t)) dt \right\}. \end{aligned}$$

Then the path q^* is the solution we want.

Theorem 1.1 (Existence and Extension Formula). *Assume $m_1 = m_3 > 0$, $m_2 = m_4 > 0$ and $\mu = \frac{m_2}{m_1}$. For any $\theta \in (0, 2\pi)$ and $\theta \notin \{\frac{\pi}{2}, \pi, \frac{3\pi}{2}\}$, there exists at least one local minimizer of $\tilde{\mathcal{A}}(\vec{a})$ over the space Γ . For any minimizer $\vec{a} \in \Gamma$ of $\tilde{\mathcal{A}}$ over the space Γ , the corresponding minimizing path $q^*(t)$ on $[0, T]$ connecting $q(0)$ and $q(T)$ can be extended to a classical solution $q(t) = (q_1(t), q_2(t), q_3(t), q_4(t))$ of the Newton's equation (2) by the reflection $B = \begin{pmatrix} -1 & 0 \\ 0 & 1 \end{pmatrix}$, the permutation σ and the rotation $R(\theta)$ as follows: $q(t) = q^*(t)$ on $[0, T]$,*

$$q(t) = (q_3^*(2T - t), q_2^*(2T - t), q_1^*(2T - t), q_4^*(2T - t))B \quad \text{on} \quad (T, 2T],$$

and

$$(7) \quad q(t) = \sigma^k(q(t - 2kT))R(-2k\theta) \text{ for } t \in (2kT, (2k + 2)T] \text{ and } k \in \mathbf{Z}^+,$$

where $\sigma = [3, 4, 1, 2]$ is a permutation such that $\sigma(q(t - 2T)) = (q_3(t - 2T), q_4(t - 2T), q_1(t - 2T), q_2(t - 2T))$.

Remark 1.2. For given (θ, μ) , there may exist more than one local minimizer other than homographic solution. But all the corresponding minimizing pathes can be extended by the same extension formula (7). For example, solutions in figure 2 are different from those solutions in figure 1 for $(\theta, \mu) = (\frac{4\pi}{5}, 0.8)$, $(\frac{4\pi}{5}, 1)$ and $(\frac{4\pi}{5}, 1.5)$. The actions of solutions in figure 2 are larger than the corresponding actions of those solutions in figure 1. By our numerical computation, solutions with smaller action seem more likely stable.

There is no loss of generality in assuming $m_1 = 1$, $\mu = \frac{m_2}{m_1}$ and $T = 1$ in numerical computation. But we still use m_1 and T for the purpose of clarity. Define $\mathcal{A}_\diamond, \mathcal{A}_{t_{path}} : (0, 2\pi) \times \mathbf{R}^+ \mapsto \mathbf{R}^+$ by

$$(8) \quad \mathcal{A}_\diamond(\theta, \mu) = 3\omega^2(m_1 r_1^2 + m_2 r_2^2)T,$$

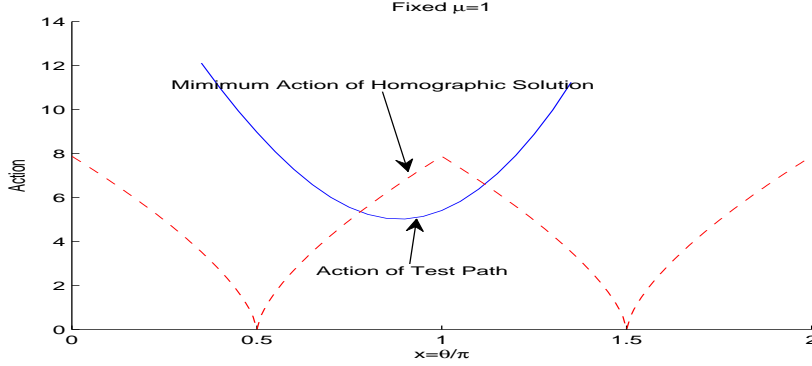


Figure 3: Fixed $\mu = 1$. The fixed SPBC $\vec{a}_{test} = [0.6676542303, 1.11499232, 0.5099504088, 0.6676542314, 1.11499232, 0.5099504078]$. Test path has lower action than homographic solution when $0.78\pi < \theta < 1.11\pi$.

where

$$(9) \quad \omega = \begin{cases} |\frac{\pi}{2} - \theta|/T, & \text{if } 0 < \theta < \pi, \\ |\frac{3\pi}{2} - \theta|/T, & \text{if } \pi \leq \theta < 2\pi. \end{cases}$$

r_1, r_2 are uniquely determined by (θ, μ) in equations (39) and (40) in section 3.1. $\mathcal{A}_\diamond(\theta, \mu)$ is the minimum value of the action functional over the homographic solution satisfying the SPBC for (θ, μ) . Now given a SPBC \vec{a}_{test} , the test path $\bar{q}(t)$ with constant velocity connecting the structural prescribed boundaries $Qstart$ and $Qend$ is given by

$$(10) \quad \bar{q}(t) = Qstart + \frac{t(Qend - Qstart)}{T}, t \in [0, T].$$

Then the action of the test path is computed as

$$(11) \quad \mathcal{A}_{tpath}(\theta, \mu) = \begin{cases} \sum_{k=1}^4 \frac{1}{2T} m_k \|Qend_k - Qstart_k\|^2 \\ + \int_0^T \sum_{1 \leq k < j \leq 4} \frac{m_k m_j}{\|(Qstart_k - Qstart_j)(1 - \frac{t}{T}) + (Qend_k - Qend_j)\frac{t}{T}\|} dt, \end{cases}$$

which is an explicit function of θ and μ . For example, fixed $\mu = 1$, figure 3 shows the graph of $\mathcal{A}_{tpath}(\theta, 1)$ and $\mathcal{A}_\diamond(\theta, 1)$. There exists an interval of θ such that test path has lower action than homographic solution has.

The set $\Omega_{\vec{a}_{test}}$ for \vec{a}_{test} is defined as

$$(12) \quad \Omega_{\vec{a}_{test}} = \{(\theta, \mu) \in (0, 2\pi) \times \mathbf{R}^+ \mid \mathcal{A}_\diamond(\theta, \mu) > \mathcal{A}_{tpath}(\theta, \mu) \text{ and } \theta \neq \pi\}.$$

The size of the set $\Omega_{\vec{a}_{test}}$ strongly depends on the choice of \vec{a}_{test} . Figure 4 shows an example of the nonempty region $\Omega_{\vec{a}_{test}}$ on which the test path has lower action than homographic solution. The admissible set Ω is defined as the union of all the set $\Omega_{\vec{a}_{test}}$.

$$(13) \quad \Omega = \bigcup_{\vec{a}_{test}} \Omega_{\vec{a}_{test}}.$$

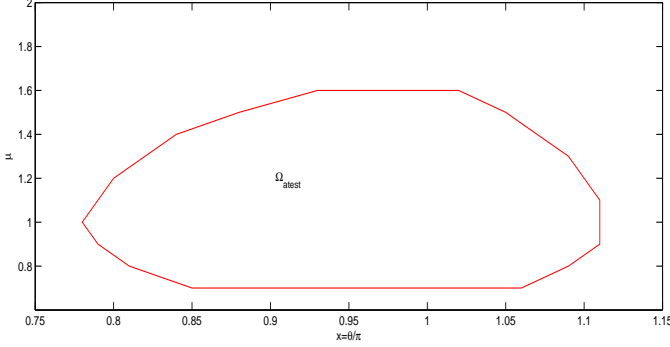


Figure 4: Test path has lower action than homographic solution when (θ, μ) is in the region $\Omega_{\vec{a}_{test}}$. The fixed SPBC $\vec{a}_{test} = [0.6676542303, 1.11499232, 0.5099504088, 0.6676542314, 1.11499232, 0.5099504078]$. The x -axis is $\frac{\theta}{\pi}$ and the y -axis is μ .

Theorem 1.3 (Classifications of Non-homographic Solutions). *For any given $(\theta, \mu) \in \Omega$ and $\theta \neq \pi$, there exists at least one minimizer $\vec{a}_0 \in \Gamma$ of $\tilde{\mathcal{A}}$ over the space Γ , such that, the corresponding minimizing path $q^*(t)$ on $[0, T]$ connecting $q(0)$ and $q(T)$ can be extended to a non-homographic solution $q(t; \theta, \mu, \vec{a}_0)$ (for short $q(t)$) of the Newton's equation (2) by the extension formula (7). Each curve $q_i(t), t \in [4kT, (4k+4)T]$ is called a side of the orbit since the orbit of the solution is assembled out the sides $q_i(t), t \in [0, 4T]$ by rotation only. The non-homographic solution $q(t; \theta, \mu, \vec{a}_0)$ can be classified as follows (see figures 8 to 14).*

- (1) **[Quasi-Periodic Solutions]** $q(t; \theta, \mu, \vec{a}_0)$ is a quasi-periodic solution if θ is not commensurable with π .
- (2) **[Periodic Solutions]** $q(t; \theta, \mu, \vec{a}_0)$ is a periodic solution if $\theta = \frac{P}{Q}\pi$, where the positive integers P and Q are relatively prime.

- When Q is even, the periodic solution $q(t; \theta, \mu, \vec{a}_0)$ is a non-choreographic solution. Each closed curve has $\frac{Q}{2}$ sides. The minimum period is $\mathcal{T} = 2QT$.

- When Q is odd, there are four cases.

Case 1: If $\mu \neq 1$, the periodic solution $q(t; \theta, \mu, \vec{a}_0)$ is a double-choreographic solution. Each closed curve has Q sides. The minimum period is $\mathcal{T} = 4QT$. Body q_1 chases body q_3 on a closed curve and body q_2 chases body q_4 on another closed curve. $q_1(t+2QT) = q_3(t)$ and $q_3(t+2QT) = q_1(t)$. $q_4(t+2QT) = q_2(t)$ and $q_2(t+2QT) = q_4(t)$.

Case 2: If $\mu = 1$ and P is odd, the periodic solution $q(t; \theta, \mu, \vec{a}_0)$ is a double-choreographic solution with minimum period $\mathcal{T} = 4QT$. Body q_1 chases body q_3 on a closed curve and body q_2 chases body q_4 on another closed curve.

Case 3: If $\mu = 1$, P is even and the initial configuration $q(0)$ is geometrically same to the ending configuration $q(T)$, i.e. $(a_{10}, a_{20}, a_{30}) = (a_{40}, a_{50}, a_{60})$, then the periodic solution is a choreographic solution. The closed curve has Q sides. The minimum period is $\mathcal{T} = 4QT$.

(A) If $\frac{Q-1}{2}$ is odd, then the four bodies chase each other on the closed curve in the order of q_1, q_2, q_3, q_4 , and then q_1 , i.e. $q_1(t+QT) = q_2(t)$, $q_2(t+QT) = q_3(t)$, $q_3(t+QT) = q_4(t)$,

and $q_4(t + QT) = q_1(t)$.

(B) If $\frac{Q-1}{2}$ is even, then the four bodies chase each other on the closed curve in the order of q_1, q_4, q_3, q_2 , and then q_1 , i.e. $q_1(t+QT) = q_4(t)$, $q_4(t+QT) = q_3(t)$, $q_3(t+QT) = q_2(t)$, and $q_2(t+QT) = q_1(t)$.

Case 4: If $\mu = 1$, P is even and the initial configuration $q(0)$ is not geometrically same to the ending configuration $q(T)$, i.e. $(a_{10}, a_{20}, a_{30}) \neq (a_{40}, a_{50}, a_{60})$, then the periodic solution is a double choreographic solution. Each closed curve has Q sides. The minimum period is $\mathcal{T} = 4QT$. Body q_1 chases body q_3 on a closed curve and body q_2 chases body q_4 on another closed curve. $q_1(t + 2QT) = q_3(t)$ and $q_3(t + 2QT) = q_1(t)$. $q_4(t + 2QT) = q_2(t)$ and $q_2(t + 2QT) = q_4(t)$.

By using canonical transformation, we reduce the dimension of the Hamiltonian system to eliminate the trivial $+1$ multipliers for the periodic solutions. Then we prove that the periodic solutions are linearly stable in the reduced system by computing the remaining multipliers of monodromy matrix. The proof is computer-assisted and it is computed one by one.

Theorem 1.4. (*Linear Stability*). Consider the solutions in theorem 1.3.

- If $\theta = \frac{2P-1}{2P}\pi$ and $\mu = 0.5, 1, 1.5$, the non-choreographic solutions $q(t)$ are linearly stable for $P = 3, 4, 5, \dots, 15$.
- If $\theta = \frac{2P}{2P+1}$ and $\mu = 0.5, 1.5$, the double choreographic solutions $q(t)$ are linearly stable for $P = 2, 3, \dots, 15$.
- If $\theta = \frac{2P-1}{2P+1}$ and $\mu = 1$, the double choreographic solutions $q(t)$ are linearly stable for $P = 4, 5, 6, \dots, 15$.
- If $\theta = \frac{2P}{2P+1}$ and $\mu = 1$, the choreographic solutions $q(t)$ are linearly stable for $P = 2, 3, 4, \dots, 15$.

Remark 1.5. (1) $\Omega_{\vec{a}_{test}}$ strongly depends on the choice of SPBC \vec{a}_{test} . The union Ω of such regions provides the range of (θ, μ) where the minimizers have lower action than the action of homographic solutions. Then new periodic or quasi-periodic solutions can be generated from these minimizers. Most solutions for $(\theta, 1)$ in theorem 1.3 have been studied in [26] but solutions for $(\theta, 1)$ in case 4 do not belong to the family of solutions in [26].

(2) Although theorem 1.3 only proves the existence of new periodic solutions for $(\theta, \mu) \in \Omega$, there exist new periodic solutions for $(\theta, \mu) \notin \Omega$. There also exist periodic solutions which have larger action than their homographic solutions have. Periodic solution with larger actions are likely unstable from our numerical simulation.

(3) We give a rigorous analytical proof for theorem 1.1 and theorem 1.3. The proof of theorem 1.4 is computer-assisted. Our theorem 1.4 and numerical simulation support the following conjecture. But the proof of the conjecture would be a quite difficult matter and it would involve some new techniques.

Conjecture: For every $(\theta, \mu) \in \Omega$ in theorem 1.3, if θ is commensurable with π , there is a linear stable periodic solution.

The rest of the paper is organized as follows. In section 2, we prove the existence and noncollision of minimizing pathes. The existence of the minimizers of the functional $\tilde{\mathcal{A}}$ over the space Γ is due to the structure of boundary conditions. Due to the collision free theorem of boundary value problem, it is not hard to prove that the corresponding path of a minimizer is collision free for all time. To prove that the initial minimizing path $q^*(t)$ in $[0, T]$ can be extended to a full solution, we have to check whether the orbits fit well at time $t = kT$. The major difficulty to construct periodic solutions in this variational method with SPBC is to find appropriate SPBC and extension formula. In section 3, we prove that the minimizer generate new periodic solutions which are not homographic orbits. A special class of homographic orbits satisfying SPBC have their configurations remaining rhomboid for all time. We study orbits of this type in section 3 and we compare them with the orbits we found. This finishes the proof of the existence of new periodic solutions other than homographic solutions. The properties of the new periodic solution are easy to prove by the extension formula. Linear stability is studied in section 4. In the last section, we list some other interesting planar 4-body SPBC and their solutions without detail proof.

2 Existence, collision free, and extension of minimizing path for boundary value problem

The minimizer is founded by a two-step minimizing process (6) with appropriate SPBC. In the first step, minimizers are obtained in the full space (4) with fixed boundary condition. For any fixed $\vec{a} \in \Gamma$, the minimizers of \mathcal{A} that connect $Qstart$ and $Qend$ are classical collision-free solutions in the interval $(0, T)$. The existence of minimizers in the Sobolev space is classic and standard. But the assertion of collision free for the boundary value problem is proved by Chenciner [7] and Marchal [22] in 2002. They proved that minimizers of \mathcal{A} on the space $\mathcal{P}(Qstart, Qend)$ are collision-free on the interval $(0, T)$ for any given $Qstart$ and $Qend$ including collision boundary. It is easy to know that $\tilde{\mathcal{A}}$ is lower semicontinuous on Γ . Then the existence of minimizers in the finite dimension space Γ is due to the following theorem.

Theorem 2.1. For $\theta \in (0, 2\pi) \setminus \{\frac{\pi}{2}, \pi, \frac{3\pi}{2}\}$, $\tilde{\mathcal{A}}(\vec{a}) \rightarrow +\infty$ if $|\vec{a}| \rightarrow +\infty$.

Proof. For any $\vec{a} \in \Gamma$,

$$\tilde{\mathcal{A}}(\vec{a}) \geq \sum_{i=1}^n \int_0^T \frac{1}{2} m_i \|\dot{q}_i(t, \vec{a})\|^2 dt \geq \sum_{i=1}^n \frac{1}{2} m_i \left\| \int_0^T \dot{q}_i(t, \vec{a}) dt \right\|^2 = \sum_{i=1}^n \frac{1}{2} m_i \|q_i(T) - q_i(0)\|^2.$$

If $|\vec{a}| \rightarrow +\infty$, then at least one $a_i \rightarrow \infty$ for $i = 1, 2, \dots, 6$. By the structural prescribed boundary conditions, $\|q_i(T) - q_i(0)\|$ can not remain finite for all i if $|\vec{a}| \rightarrow +\infty$.

In fact, if $a_1 \rightarrow \infty$ or $a_2 \rightarrow \infty$, $\tilde{\mathcal{A}}(\vec{a}) \geq \frac{1}{2} m_2 \|q_2(T) - q_2(0)\|^2 + \frac{1}{2} m_4 \|q_4(T) - q_4(0)\|^2 > \frac{1}{2} m_2 |a_1 \cos(\theta) - a_2 \sin(\theta)| + \frac{1}{2} m_4 |a_1 \cos(\theta) + a_2 \sin(\theta)| \rightarrow \infty$ since $\theta \neq \frac{\pi}{2}$, $\theta \neq \pi$ and $\theta \neq \frac{3\pi}{2}$.

If $a_3 \rightarrow \infty$, $\tilde{\mathcal{A}}(\vec{a}) \geq \frac{1}{2} m_1 \|q_1(T) - q_1(0)\|^2 + \frac{1}{2} m_3 \|q_3(T) - q_3(0)\|^2 > \frac{1}{2} m_1 |a_3 \sin(\theta) + a_4| + \frac{1}{2} m_3 \left| \frac{-m_2 a_2 - m_4 a_2 + m_1 a_3}{m_3} \sin(\theta) - a_4 \right| \rightarrow \infty$ for any choice of a_4 . Other cases can be easily obtained by similar arguments.

□

Theorem 2.2 (Collision-free). *For $\theta \in (0, 2\pi) \setminus \{\frac{\pi}{2}, \pi, \frac{3\pi}{2}\}$, let \vec{a}_0 be a minimizer of $\tilde{\mathcal{A}}(\vec{a})$ over the space Γ and the corresponding path $q^*(t) \in S(\vec{a}_0)$. Then q^* satisfying SPBC is a classical collision-free solution of Newton's equation (2) in the whole interval $[0, T]$.*

Proof. If \vec{a}_0 is a minimizer of $\tilde{\mathcal{A}}(\vec{a})$ over the space Γ , it is well known that the corresponding path $q^*(t)$ is collision-free in the open interval $(0, T)$. To prove q^* is a classical solution of Newton's equation in the whole interval $[0, T]$, we only need to prove that $Qstart(a_{10}, a_{20}, a_{30})$ and $Qend(a_{40}, a_{50}, a_{60})$ have no collision. In fact, there are six cases corresponding to initial collision boundary. (1) $a_{10} \neq 0$ and $a_{20} = \mu^{-1}a_{30}$ binary collision (m_1 and m_3 collide). (2) $a_{10} = 0$, $a_{20} \neq -a_{30}$, $a_{20} \neq \mu^{-1}a_{30}$ and $a_{20} \neq \frac{1}{1+2\mu}a_{30}$, binary collision (m_2 and m_4 collide). (3) $a_{10} = 0$, and $a_{20} = \mu^{-1}a_{30} \neq 0$ simultaneous binary collision (m_1 and m_3 collide and m_2 and m_4 collide). (4) $a_{10} = a_{20} = a_{30} = 0$ total collision. (5) $a_{10} = 0$, $a_{20} = -a_{30} \neq 0$ triple collision (m_1 , m_2 , and m_4 collide). (6) $a_{10} = 0$, $a_{20} = \frac{1}{1+2\mu}a_{30} \neq 0$ triple collision (m_2 , m_3 , and m_4 collide). Similarly, there are six cases corresponding to ending collision boundary.

Since q has no collision in the open interval $(0, T)$, we will then analyze the motion during the closed time interval $[0, \epsilon]$ or $[\epsilon, T]$ and prove the existence of sufficiently small values of ϵ such that a local deformation has lower action and satisfy the SPBC. The contradiction proves that q can not have this collision. Local deformation argument has appeared in a number of papers such as Chenciner [7], Chen [13], Ferrario-Terracini [17], Marchal [22], and Terracini-Venturelli [34] etc. Here we only study the collisions at $t = 0$ and similar arguments can be applied for collisions at $t = T$. By the nature of SPBC and the construction of the local deformation, we will prove it in two cases: collision with two bodies and collision with three or more bodies. The proof is almost the same as the proof in the paper by Ouyang-Xie [26] except the perturbation on the deformation due to the differences of SPBC. We include here for the sake of completeness.

CASE ONE: Collision with two bodies.

Suppose that q is a local minimizer of \mathcal{A} satisfying the SPBC for \vec{a}_0 . Let the collision subset $\mathcal{C} = \{\tau_1, \tau_2\} \subseteq \{1, 2, 3, 4\}$. At time $t = 0$, the bodies m_{τ_1} and m_{τ_2} start at the collision point $q_{\tau_1}(0) = q_{\tau_2}(0)$ while the other bodies are away. By the structural of SPBC, the collision set \mathcal{C} must be either $\{1, 3\}$ or $\{2, 4\}$ which is corresponding to the binary collisions (1), (2) and (3) at $t = 0$.

We will build the two following pathes S_2 (Kepler ejection orbits at the starting point) and S_3 (the deformation of S_2) with: (A) Exactly the same motion of all bodies in the interval $[\epsilon, T]$. (B) At the time interval $[0, \epsilon]$, the ejection orbits are replaced by a collision free orbits with boundary conditions satisfying SPBC. The corresponding actions will be $A_1 = \mathcal{A}(q)$, $A_2 = \mathcal{A}(S_2)$, $A_3 = \mathcal{A}(S_3)$. We want to prove that $A_1 > A_3$ for sufficiently small time ϵ . Since (A), the actions are different only in the time interval $[0, \epsilon]$.

First, consider the ejection orbits in the starting time interval $[0, \epsilon]$ in S_2 . Let r be the simple radial two-body motion leading from 0 to r_ϵ in the time interval $[0, \epsilon]$. By Sundman and Sperling's estimates near collisions [31, 32], there exists a positive constant γ such that $r(t) = (\gamma t^{\frac{2}{3}})\vec{\alpha}$ where $\vec{\alpha}$ is a unit vector. Let $\xi(t) = \frac{m_{\tau_1}q_{\tau_1}(t) + m_{\tau_2}q_{\tau_2}(t)}{m_{\tau_1} + m_{\tau_2}}$ be the center of mass of

the τ_1 -th and τ_2 -th bodies.

$$q_{\tau_1 S_2}(t) = \xi(t) + \frac{m_{\tau_2}}{m_{\tau_1} + m_{\tau_2}} r(t), q_{\tau_2 S_2}(t) = \xi(t) - \frac{m_{\tau_1}}{m_{\tau_1} + m_{\tau_2}} r(t);$$

$$q_j S_2(t) = q_j(t), j \notin \mathcal{C}.$$

We consider the deformation of $r(t)$ as

$$(14) \quad r_\delta(t) = r(t) + \delta \phi(t) \vec{s},$$

where \vec{s} is an appropriate unit vector, $\delta = \frac{\epsilon}{N}$ with $N \geq 2 \max\{K_{in}/U_{in}, 4\}$, and

$$\phi(t) = \begin{cases} 1, & 0 \leq t \leq \delta, \\ \frac{\delta + \tilde{N}\delta - t}{N\delta}, & \delta < t \leq \delta + \tilde{N}\delta, \\ 0, & \delta + \tilde{N}\delta < t \leq \epsilon, \end{cases}$$

where $K_{in}/U_{in} < \tilde{N} < N - 1$. The positive K_{in} and U_{in} are given in the equations (22) and (23) respectively, which are independent of ϵ .

The collision-free motion S_3 is denoted by

$$q_{\tau_1 S_3}(t) = \xi(t) + \frac{m_{\tau_2}}{m_{\tau_1} + m_{\tau_2}} r_\delta(t), q_{\tau_2 S_3}(t) = \xi(t) - \frac{m_{\tau_1}}{m_{\tau_1} + m_{\tau_2}} r_\delta(t);$$

$$q_j S_3(t) = q_j(t), j \notin \mathcal{C}.$$

We choose \vec{s} to be the unit vector of $(0, \pm 1)R(\theta)$ when $\{\tau_1, \tau_2\} = \{2, 4\}$ and we choose \vec{s} to be the unit vector of $(\pm 1, 0)R(\theta)$ when $\{\tau_1, \tau_2\} = \{1, 3\}$. The sign will be determined later. So the initial condition of S_3 satisfies the SPBC.

Now consider the expression of the actions for each path in the time interval $[0, \epsilon]$. They will be decomposed into two parts: the first part A_{in} is to compute the action of the relative motion of the colliding bodies m_{τ_1} and m_{τ_2} ; the second part A_{out} is to compute the action of the remainder. It is easy to know that $A_{1in} \geq A_{2in}$ since the homothetic collision-ejection orbit is a minimizer. We only need to prove $A_{2in} - A_{3in} > A_{3out} - A_{1out}$ in order to prove $A_1 > A_3$ in $[0, \epsilon]$. We first note that

$$\begin{aligned} m_{\tau_1} |\dot{q}_{\tau_1 S_2}|^2 + m_{\tau_2} |\dot{q}_{\tau_2 S_2}|^2 &= m_{\tau_1} \left\langle \dot{\xi} + \frac{m_{\tau_2}}{m_{\tau_1} + m_{\tau_2}} \dot{r}, \dot{\xi} + \frac{m_{\tau_2}}{m_{\tau_1} + m_{\tau_2}} \dot{r} \right\rangle + \\ m_{\tau_2} \left\langle \dot{\xi} - \frac{m_{\tau_1}}{m_{\tau_1} + m_{\tau_2}} \dot{r}, \dot{\xi} - \frac{m_{\tau_1}}{m_{\tau_1} + m_{\tau_2}} \dot{r} \right\rangle &= (m_{\tau_1} + m_{\tau_2}) |\dot{\xi}|^2 + \frac{m_{\tau_1} m_{\tau_2}}{m_{\tau_1} + m_{\tau_2}} |\dot{r}|^2. \end{aligned}$$

Then

$$A_{2in} - A_{3in} = \int_0^\epsilon \frac{m_{\tau_1} m_{\tau_2}}{2(m_{\tau_1} + m_{\tau_2})} (|\dot{r}|^2 - |\dot{r}_\delta|^2) + m_{\tau_1} m_{\tau_2} \left(\frac{1}{|r|} - \frac{1}{|r_\delta|} \right) dt,$$

$$A_{3out} - A_{1out} = \int_0^\epsilon \sum_{i \notin \mathcal{C}; \tau_j \in \mathcal{C}} \left(\frac{m_i m_{\tau_j}}{|q_i - q_{\tau_j S_3}|} - \frac{m_i m_{\tau_j}}{|q_i - q_{\tau_j}|} \right) dt.$$

Now we estimate the bounds for A_{out} . Consider the motion of the mass m_j between the arbitrary successive instants t_1 and t_2 . Because the minimum of the integral $\int_{t_1}^{t_2} \frac{m_j |\dot{q}_j|^2}{2} dt$ between given positions $q_j(t_1)$ and $q_j(t_2)$ is obtained for a constant velocity vector, we can always write $\frac{m_j |q_j(t_2) - q_j(t_1)|^2}{2(t_2 - t_1)} \leq \int_{t_1}^{t_2} \frac{m_j |\dot{q}_j|^2}{2} dt \leq \mathcal{A}(q) \leq K < \infty$. So if $0 \leq t_1 \leq t_2 \leq T$, $|q_j(t_2) - q_j(t_1)| \leq \left(\frac{2K(t_2 - t_1)}{m_j} \right)^{1/2}$. Pick up $\epsilon > 0$ small such that the two bodies m_{τ_1} and m_{τ_2} will remain at less than twice that distance from the collision point $q_{\tau_1}(0)$ all along the time interval $[0, \epsilon]$, i.e. $|q_{\tau_1} - q_{\tau_2}| \leq J\sqrt{\epsilon}$, where $J = 2(2K)^{1/2}$. $m_j, j \notin \mathcal{C}$ will remain outside of the circle centered at the collision point with radius D and $J\sqrt{\epsilon} \leq J\sqrt{\epsilon_0} \ll D$ for a fixed ϵ_0 . So during the time interval $[0, \epsilon]$, the bodies $m_j, j \notin \mathcal{C}$ are outside of the circle with radius D and center $q_{\tau_1}(0)$, while the bodies m_{τ_1} and m_{τ_2} are inside the much smaller circle of the same center and radius $J\sqrt{\epsilon}$.

$$\begin{aligned}
|A_{3out} - A_{1out}| &\leq \int_0^\epsilon \sum_{i \notin \mathcal{C}; \tau_j \in \mathcal{C}} m_i m_{\tau_j} \left| \left(\frac{|q_i - q_{\tau_j} S_3| - |q_i - q_{\tau_j}|}{|q_i - q_{\tau_j}| |q_i - q_{\tau_j} S_3|} \right) \right| dt. \\
&\leq \int_0^\epsilon \sum_{i \notin \mathcal{C}; j \in \mathcal{C}} m_i m_{\tau_j} \left(\frac{|q_{\tau_j} S_3 - q_{\tau_j}|}{|q_i - q_{\tau_j}| |q_i - q_{\tau_j} S_3|} \right) dt. \\
(15) \quad &\leq \int_0^\epsilon \sum_{i \notin \mathcal{C}; \tau_j \in \mathcal{C}} m_i m_{\tau_j} \left(\frac{J\sqrt{\epsilon}}{(D - J\sqrt{\epsilon_0})^2} \right) dt = \frac{4J}{(D - J\sqrt{\epsilon_0})^2} \epsilon^{\frac{3}{2}} = U_{out} \epsilon^{\frac{3}{2}}.
\end{aligned}$$

Let us compute $A_{2in} - A_{3in}$. By choosing appropriate direction of \vec{s} such that $\langle r, \vec{s} \rangle \geq 0$,

$$\begin{aligned}
&\int_0^\epsilon \frac{m_{\tau_1} m_{\tau_2}}{2(m_{\tau_1} + m_{\tau_2})} (|\dot{r}|^2 - |\dot{r}_\delta|^2) dt = - \int_0^\epsilon \frac{m_{\tau_1} m_{\tau_2}}{2(m_{\tau_1} + m_{\tau_2})} (2\delta \dot{\phi} \langle r, \vec{s} \rangle + (\delta \dot{\phi})^2) dt \\
&\geq - \int_\delta^{\delta + \tilde{N}\delta} \frac{m_{\tau_1} m_{\tau_2}}{2(m_{\tau_1} + m_{\tau_2})} (\delta \dot{\phi})^2 dt = - \int_\delta^{\delta + \tilde{N}\delta} \frac{m_{\tau_1} m_{\tau_2}}{2(m_{\tau_1} + m_{\tau_2})} \left(-\frac{1}{\tilde{N}} \right)^2 dt \\
(16) \quad &\geq - \frac{m_{\tau_1} m_{\tau_2}}{2(m_{\tau_1} + m_{\tau_2})} \frac{\delta}{\tilde{N}} = -K_{in} \frac{\delta}{\tilde{N}}.
\end{aligned}$$

$$\begin{aligned}
&\int_0^\epsilon \left(\frac{1}{|r|} - \frac{1}{|r_\delta|} \right) dt = \int_0^\epsilon \left(\frac{1}{|r|} - \frac{1}{(|r|^2 + 2\delta \phi \langle r, \vec{s} \rangle + (\delta \phi)^2)^{1/2}} \right) dt \\
&= \int_0^\epsilon \left(\frac{2\delta \phi \langle r, \vec{s} \rangle + (\delta \phi)^2}{|r| (|r|^2 + 2\delta \phi \langle r, \vec{s} \rangle + (\delta \phi)^2)^{1/2} (|r| + (|r|^2 + 2\delta \phi \langle r, \vec{s} \rangle + (\delta \phi)^2)^{1/2})} \right) dt \\
&\geq \int_0^\delta \left(\frac{(\delta)^2}{|r| (|r| + \delta) (2|r| + \delta)} \right) dt \geq \int_0^\delta \left(\frac{1}{\gamma(\gamma + \delta^{1/3})(2\gamma + \delta^{1/3})} \right) dt \\
(17) \quad &\geq \left(\frac{1}{\gamma(\gamma + 1)(2\gamma + 1)} \right) \delta = U_{in} \delta,
\end{aligned}$$

where we use the fact $|r| \leq \gamma\delta^{2/3}$ in $[0, \delta]$ and $\delta < 1$.

So $A_{2in} - A_{3in} > \left(-K_{in}\frac{\delta}{N} + U_{in}\delta\right) = \left(-\frac{K_{in}}{N} + U_{in}\right)\frac{\epsilon}{N} > U_{out}\epsilon^{\frac{3}{2}} \geq A_{3out} - A_{1out}$ for small ϵ , which implies $A_1 > A_3$.

The action of S_3 is smaller than the action of S_1 which contradicts the fact that S_1 is a minimizer. The contradiction completes the proof that the vector \vec{a}_0 with binary collision is not a minimizer of \mathcal{A} on Γ .

CASE TWO: Collisions with three or more bodies.

We can give a unify proof as we did in paper [26]. But for the sake of clarity and simplicity, we only prove the triple collision case (5) $a_{10} = 0, a_{20} = -a_{30} \neq 0$, where m_1, m_2 , and m_4 collide while m_3 is away. We will build the two similar solutions S_2 (Kepler ejection orbits at the starting point) and S_3 (deformation of S_2) as we built for binary collisions. First, consider the ejection orbits in the starting time interval $[0, \epsilon]$ in S_2 . By [27, 31], the configuration of the colliding bodies m_1, m_2, m_4 is approaching the set of central configurations. Let $\bar{\omega} = (\bar{\omega}_1, \bar{\omega}_2, \bar{\omega}_4)$ be the translation of the central configuration $(q_1(\epsilon), q_2(\epsilon), q_4(\epsilon))$ by shifting center of mass at origin. By Sundman and Sperling's estimates near collisions [31, 32], the homothetic collision-ejection orbit is given by $\omega_i(t) = \bar{\omega}_i t^{2/3}$, $i = 1, 2, 4$ and $t \in [0, \epsilon]$. Let $\xi(t) = \frac{m_1 q_1(t) + m_2 q_2(t) + m_4 q_4(t)}{m_1 + m_2 + m_4}$ be the center of mass of the colliding bodies.

$$q_{1S_2}(t) = \xi(t) + \omega_1(t), q_{2S_2}(t) = \xi(t) + \omega_2(t),$$

$$q_{3S_2}(t) = q_3(t), q_{4S_2}(t) = \xi(t) + \omega_4(t).$$

We consider the deformation of $\omega_i(t)$ as

$$(18) \quad \omega_{1\delta}(t) = \omega_1(t) - \frac{1}{m_1}\delta\phi(t)\vec{s}_1,$$

$$(19) \quad \omega_{2\delta}(t) = \omega_2(t) + \frac{1}{2m_2}\delta\phi(t)\vec{s}_1 + \frac{1}{2m_2}\delta\phi(t)\vec{s}_2,$$

$$(20) \quad \omega_{4\delta}(t) = \omega_4(t) + \frac{1}{2m_4}\delta\phi(t)\vec{s}_1 - \frac{1}{2m_4}\delta\phi(t)\vec{s}_2,$$

where \vec{s}_1, \vec{s}_2 are two appropriate unit vectors of $(0, \pm 1)R(\theta)$ or $(\pm 1, 0)R(\theta)$, $\delta = \frac{\epsilon}{N}$ with $N \geq 2 \max\{K_{in}/U_{in}, 4\}$, and

$$\phi(t) = \begin{cases} 1, & 0 \leq t \leq \delta, \\ \frac{\delta + \tilde{N}\delta - t}{N\delta}, & \delta < t \leq \delta + \tilde{N}\delta, \\ 0, & \delta + \tilde{N}\delta < t \leq \epsilon. \end{cases}$$

where $K_{in}/U_{in} < \tilde{N} < N - 1$. The positive K_{in} and U_{in} are constants given in the equations (22) and (23) respectively. The deformation S_3 is denoted by

$$q_{1S_3}(t) = \xi(t) + \omega_{1\delta}(t), q_{2S_3}(t) = \xi(t) + \omega_{2\delta}(t),$$

$$q_{3S_3}(t) = q_3(t), q_{4S_3}(t) = \xi(t) + \omega_{4\delta}(t).$$

At $t = 0$, $q_{1S_3}(0) = (0, -a_{30} \pm \delta/m_1)R(\theta)$, $q_{2S_3}(0) = (\pm\delta/m_2, -a_{30} \mp \delta/(2m_2))R(\theta)$, $q_{3S_3}(0) = (0, (2\mu + 1)a_{30})R(\theta)$, $q_{4S_3}(0) = (\mp\delta/m_4, -a_{30} \mp \delta/(2m_4))R(\theta)$. So the initial conditions of S_3 satisfy the SPBC.

Now consider the expression of the actions for each path in the time interval $[0, \epsilon]$. They will be decomposed into two parts: the first part A_{in} is to compute the action of the relative motion of the colliding bodies m_1 , m_2 and m_4 ; the second part A_{out} is to compute the action of the remainder.

It is easy to know that $A_{1in} \geq A_{2in}$ since the homothetic collision-ejection orbit is a minimizer. We only need to prove $A_{2in} - A_{3in} > A_{3out} - A_{1out}$ in order to prove $A_1 > A_3$ in $[0, \epsilon]$.

First of all, we estimate $A_{3out} - A_{1out}$. Consider the motion of the mass m_j between the arbitrary successive instants t_1 and t_2 . Because the minimum of the integral $\int_{t_1}^{t_2} \frac{m_j |\dot{q}_j|^2}{2} dt$ between given positions $q_j(t_1)$ and $q_j(t_2)$ is obtained for a constant velocity vector, we can always write $\frac{m_j |q_j(t_2) - q_j(t_1)|^2}{2(t_2 - t_1)} \leq \int_{t_1}^{t_2} \frac{m_j |\dot{q}_j|^2}{2} dt \leq \mathcal{A}(q) \leq K < \infty$. So if $0 \leq t_1 \leq t_2 \leq T$, $|q_j(t_2) - q_j(t_1)| \leq \left(\frac{2K(t_2 - t_1)}{m_j}\right)^{1/2}$. Pick up $\epsilon > 0$ small such that the three bodies m_1 , m_2 and m_4 will remain in a circle with radius $J\sqrt{\epsilon}$ from the collision point $(0, -a_{30})$ all along the time interval $[0, \epsilon]$, i.e. where $J = (2K/\min\{m_i\})^{1/2}$. Then $|q_i - q_j| \leq 2J\sqrt{\epsilon}$ for $i, j = 1, 2, 4$. m_3 will remain outside of the circle centered at the collision point with radius D and $J\sqrt{\epsilon} \leq J\sqrt{\epsilon_0} \ll D$. So during the time interval $[0, \epsilon]$, the body m_3 is outside of the circle with radius D and center $(0, -a_{30})$, while the bodies m_1 , m_2 and m_4 are inside the much smaller circle with the same center and radius $J\sqrt{\epsilon}$.

$$\begin{aligned} |A_{3out} - A_{1out}| &= \left| \int_0^\epsilon \frac{1}{2} m_3 |\dot{q}_{3S_3}(t)|^2 - \frac{1}{2} m_3 |\dot{q}_3(t)|^2 + \sum_{i=1,2,4} \frac{m_i m_3}{|q_{iS_3} - q_{3S_3}|} - \frac{m_i m_3}{|q_i - q_3|} dt \right| \\ &= \left| \int_0^\epsilon \sum_{i=1,2,4} \frac{m_i m_3 (|q_i - q_3| - |q_{iS_3} - q_{3S_3}|)}{|q_{iS_3} - q_{3S_3}| |q_i - q_3|} dt \right| \leq \int_0^\epsilon \sum_{i=1,2,4} \frac{m_i m_3 (|q_i - q_{iS_3}|)}{|q_{iS_3} - q_{3S_3}| |q_i - q_3|} dt \\ (21) \quad &\leq \int_0^\epsilon \frac{2M m_3 J \sqrt{\epsilon}}{(D - J\sqrt{\epsilon})^2} dt \leq \frac{2M m_3 J \epsilon^{3/2}}{(D - J\sqrt{\epsilon_0})^2} = U_{out} \epsilon^{3/2}. \end{aligned}$$

Now we compute

$$A_{2in} - A_{3in} = \int_0^\epsilon \sum_{i=1,2,4} \frac{1}{2} m_i (|\dot{q}_{iS_2}|^2 - |\dot{q}_{iS_3}|^2) + \sum_{i < j=1,2,4} \frac{m_i m_j}{|q_{iS_2} - q_{jS_2}|} - \frac{m_i m_j}{|q_{iS_3} - q_{jS_3}|} dt.$$

Because $m_2 = m_4$ and $\omega_i(t) - \omega_j(t) = (\bar{\omega}_i - \bar{\omega}_j)t^{2/3}$ in $[0, \epsilon]$, we are able to pick up the appropriate direction vector \vec{s}_1 and \vec{s}_2 such that the inner product

$$\langle \omega_2(t) - \omega_4(t), \left(\frac{1}{2m_2} + \frac{1}{2m_4} \right) \delta\phi(t) \vec{s}_2 \rangle \geq 0$$

and

$$\langle \omega_2(t) - \omega_1(t), \left(\frac{1}{2m_2} + \frac{1}{m_1} \right) \delta\phi(t)\vec{s}_1 + \left(\frac{1}{2m_2} \right) \delta\phi(t)\vec{s}_2 \rangle \geq 0.$$

Because $\bar{\omega}_1$, $\bar{\omega}_2$, and $\bar{\omega}_4$ is a central configuration, they are either collinear or equilateral triangle. So

$$\langle \omega_4(t) - \omega_1(t), \left(\frac{1}{2m_4} + \frac{1}{m_1} \right) \delta\phi(t)\vec{s}_1 - \left(\frac{1}{2m_4} \right) \delta\phi(t)\vec{s}_2 \rangle \geq 0.$$

Since both the centers of mass of central configurations $\omega(t)$ and $\omega_\delta(t)$ are at origin, we have the kinetic energy

$$\sum_{i=1,2,4} \frac{1}{2} m_i |\dot{q}_{iS_2}|^2 = \sum_{i=1,2,4} \frac{1}{2} m_i (|\dot{\xi}|^2 + |\dot{\omega}_i(t)|^2) \text{ and } \sum_{i=1,2,4} \frac{1}{2} m_i |\dot{q}_{iS_3}|^2 = \sum_{i=1,2,4} \frac{1}{2} m_i (|\dot{\xi}|^2 + |\dot{\omega}_{i\delta}(t)|^2).$$

$$\begin{aligned} \int_0^\epsilon \sum_{i=1,2,4} \frac{1}{2} m_i (|\dot{q}_{iS_2}|^2 - |\dot{q}_{iS_3}|^2) dt &= \int_0^\epsilon \sum_{i=1,2,4} \frac{1}{2} m_i (|\dot{\omega}_i(t)|^2 - |\dot{\omega}_{i\delta}(t)|^2) dt \\ &\geq - \int_\delta^{\delta + \tilde{N}\delta} \frac{1}{2} m_1 \left| \frac{1}{m_1} \delta\dot{\phi}(t)\vec{s}_1 \right|^2 + \frac{1}{2} m_2 \left| \frac{1}{2m_2} \delta\dot{\phi}(t)\vec{s}_1 + \frac{1}{2m_2} \delta\dot{\phi}(t)\vec{s}_2 \right|^2 \\ &\quad + \frac{1}{2} m_4 \left| \frac{1}{2m_4} \delta\dot{\phi}(t)\vec{s}_1 - \frac{1}{2m_4} \delta\dot{\phi}(t)\vec{s}_2 \right|^2 dt \\ (22) \quad &\geq - \left(\frac{1}{2m_1} + \frac{1}{4m_2} + \frac{1}{4m_4} \right) \left(\frac{\delta}{\tilde{N}} \right) \equiv -K_{in} \frac{\delta}{\tilde{N}}. \end{aligned}$$

Let $m_{12} = \left(\left(\frac{1}{m_1} + \frac{1}{2m_2} \right)^2 + \frac{1}{4m_2^2} \right)^{\frac{1}{2}}$. For potential energy, we have

$$\begin{aligned} &\int_0^\epsilon \sum_{i < j = 1, 2, 4} \frac{m_i m_j}{|q_{iS_2} - q_{jS_2}|} - \frac{m_i m_j}{|q_{iS_3} - q_{jS_3}|} dt = \\ &= \int_0^\epsilon \sum_{i < j = 1, 2, 4} m_i m_j \frac{|\omega_{i\delta}(t) - \omega_{j\delta}(t)| - |\omega_i(t) - \omega_j(t)|}{|\omega_i(t) - \omega_j(t)| |\omega_{i\delta}(t) - \omega_{j\delta}(t)|} \\ &\geq \int_0^\epsilon \sum_{i < j = 1, 2, 4} \frac{m_i m_j |\omega_{i\delta} - \omega_i + \omega_j - \omega_{j\delta}|^2}{|\omega_i(t) - \omega_j(t)| |\omega_{i\delta}(t) - \omega_{j\delta}(t)| (|\omega_{i\delta}(t) - \omega_{j\delta}(t)| + |\omega_i(t) - \omega_j(t)|)} dt \\ &\geq \int_0^\epsilon \frac{m_1 m_2 |\omega_{1\delta} - \omega_1 + \omega_2 - \omega_{2\delta}|^2}{|\omega_1(t) - \omega_2(t)| |\omega_{1\delta}(t) - \omega_{2\delta}(t)| (|\omega_{1\delta}(t) - \omega_{2\delta}(t)| + |\omega_1(t) - \omega_2(t)|)} dt \\ &\geq \int_0^\delta \frac{m_1 m_2 m_{12}^2 \delta^2}{|\omega_1(t) - \omega_2(t)| |\omega_{1\delta}(t) - \omega_{2\delta}(t)| (|\omega_{1\delta}(t) - \omega_{2\delta}(t)| + |\omega_1(t) - \omega_2(t)|)} dt \\ &\geq \int_0^\delta \frac{m_1 m_2 m_{12}^2}{|\bar{\omega}_1 - \bar{\omega}_2| (|\bar{\omega}_1 - \bar{\omega}_2| + m_{12} \delta^{1/3}) (2|\bar{\omega}_1 - \bar{\omega}_2| + m_{12} \delta^{1/3})} dt \end{aligned}$$

$$(23) \quad \geq \frac{m_1 m_2 m_{12}^2}{|\bar{\omega}_1 - \bar{\omega}_2| (|\bar{\omega}_1 - \bar{\omega}_2| + m_{12}) (2|\bar{\omega}_1 - \bar{\omega}_2| + m_{12})} \delta \equiv U_{in} \delta.$$

From the above estimations (21),(22) and (23), by picking small enough ϵ , we have

$$A_{2in} - A_{3in} \geq \left(U_{in} - \frac{K_{in}}{\tilde{N}} \right) \delta = \left(U_{in} - \frac{K_{in}}{\tilde{N}} \right) \frac{\epsilon}{N} \geq U_{out} \epsilon^{3/2} > A_{3out} - A_{1out}.$$

This completes the proof that the minimizer can not have the triple collision. □

Let \mathbf{A} and \mathbf{B} be two proper linear subspaces of $(\mathbf{R}^2)^4$ which are given as

$$\mathbf{A} = \left\{ \left(\begin{array}{cc} 0 & -a_3 \\ -a_1 & a_2 \\ 0 & \frac{-m_2 a_2 - m_4 a_2 + m_1 a_3}{m_3} \\ a_1 & a_2 \end{array} \right) \in (\mathbf{R}^2)^4 \mid (a_1, a_2, a_3) \in \mathbf{R}^3 \right\}$$

and

$$\mathbf{B} = \left\{ \left(\begin{array}{cc} a_4 & a_5 \\ 0 & -a_6 \\ -a_4 & a_5 \\ 0 & \frac{-m_1 a_5 - m_3 a_5 + m_2 a_6}{m_4} \end{array} \right) \in (\mathbf{R}^2)^4 \mid (a_4, a_5, a_6) \in \mathbf{R}^3 \right\}.$$

Let us consider the action functional \mathcal{A} defined in (1) over the function space

$$\mathcal{P}(\mathbf{A}, \mathbf{B}) := \{q \in H^1([0, T], (\mathbf{R}^2)^4) \mid q(0) \in \mathbf{A}, q(T) \in \mathbf{B}\}.$$

It is easy to prove the theorem of equivalence below.

Theorem 2.3 (Equivalence). *$\vec{a}_0 \in \Gamma$ with corresponding path $q^* \in S(\vec{a}_0)$ satisfying $q^*(0) = Q_{start}$ and $q^*(T) = Q_{end}$ is a minimizer of $\hat{\mathcal{A}}(\vec{a})$ over the space Γ , if and only if, q^* is a minimizer of \mathcal{A} over the function space $\mathcal{P}(\mathbf{A}, \mathbf{B})$ with $q^*(0) = Q_{start} \in \mathbf{A}$ and $q^*(T) = Q_{end} \in \mathbf{B}$.*

Now it is ready to prove theorem 1.1.

Proof of Theorem 1.1. By theorem 2.2, any path $q^*(t)$ corresponding to a local minimizer \vec{a}_0 is a classic solution in the interval $[0, T]$. We only need to prove that it can be extended to a classical solution by the extension formula (7).

Because $q^*(t)$ is a classic solution of Newton's equation (2) on $[0, T]$, it is easy to check that $q(t)$ is a classical solution in each interval $((n-1)T, nT)$ for any given positive integer n . To prove $q(t)$ is a classical solution for all real t , we need to prove that $q(t)$ is connected very well at $t = nT$ for any integer n , i.e. $\lim_{t \rightarrow (nT)^-} q(t) = \lim_{t \rightarrow (nT)^+} q(t)$ and $\lim_{t \rightarrow (nT)^-} \dot{q}(t) = \lim_{t \rightarrow (nT)^+} \dot{q}(t)$. By the structure of the extension equation (7), we only need prove it for $n = 1$ and $n = 2$.

By the SPBC, at $n = 1$, we have $\lim_{t \rightarrow (T)^-} q(t) = \lim_{t \rightarrow (T)^+} q(t)$ because

$$\lim_{t \rightarrow (T)^-} q(t) = (q_1^*(T), q_2^*(T), q_3^*(T), q_4^*(T)) = Q_{end},$$

and

$$\lim_{t \rightarrow (T)^+} q(t) = (q_3^*(T), q_2^*(T), q_1^*(T), q_4^*(T)) B = Q_{end}.$$

At $n = 2$, we have $\lim_{t \rightarrow (2T)^-} q(t) = \lim_{t \rightarrow (2T)^+} q(t)$ because

$$\lim_{t \rightarrow (2T)^-} q(t) = (q_3^*(0), q_2^*(0), q_1^*(0), q_4^*(0)) B = \begin{pmatrix} 0 & \frac{-m_2 a_2 - m_4 a_2 + m_1 a_3}{m_3} \\ -a_1 & a_2 \\ 0 & -a_3 \\ a_1 & a_2 \end{pmatrix} R(\theta) B,$$

and

$$\lim_{t \rightarrow (2T)^+} q(t) = (q_3^*(0), q_4^*(0), q_1^*(0), q_2^*(0)) R(-2\theta) = \begin{pmatrix} 0 & \frac{-m_2 a_2 - m_4 a_2 + m_1 a_3}{m_3} \\ a_1 & a_2 \\ 0 & -a_3 \\ -a_1 & a_2 \end{pmatrix} R(-\theta).$$

That $\lim_{t \rightarrow (nT)^-} \dot{q}(t) = \lim_{t \rightarrow (nT)^+} \dot{q}(t)$ at $n = 1$ and $n = 2$ is equivalent to the relations given by (24) and (25) below. At $t = T$,

$$(24) \quad \dot{q}_{11}(T) = \dot{q}_{31}(T), \dot{q}_{12}(T) = -\dot{q}_{32}(T), \dot{q}_{22}(T) = \dot{q}_{42}(T) = 0,$$

and at $t = 2T$,

$$(25) \quad \begin{aligned} \dot{q}_1(0) &= (\dot{q}_{11}(0), -\dot{q}_{12}(0)) R(2\theta), & \dot{q}_2(0) &= (\dot{q}_{41}(0), -\dot{q}_{42}(0)) R(2\theta), \\ \dot{q}_3(0) &= (\dot{q}_{31}(0), -\dot{q}_{32}(0)) R(2\theta), & \dot{q}_4(0) &= (\dot{q}_{21}(0), -\dot{q}_{22}(0)) R(2\theta). \end{aligned}$$

Now we prove the equalities (24) and (25). Since $\vec{a}_0 \in \Gamma$ is a minimizer of $\tilde{\mathcal{A}}(\vec{a})$ over Γ , q^* is a minimizer of \mathcal{A} over the function space $\mathcal{P}(\mathbf{A}, \mathbf{B})$ by theorem 2.3. Here we use q for q^* by our extension formula (7). Consider an admissible variation $\xi \in \mathcal{P}(\mathbf{A}, \mathbf{B})$ with $\xi(0) \in \mathbf{A}$ and $\xi(T) \in \mathbf{B}$, then the first variation $\delta_\xi \mathcal{A}(q)$ is computed as:

$$\begin{aligned} \delta_\xi \mathcal{A}(q) &= \lim_{\delta \rightarrow 0} \frac{\mathcal{A}(q + \delta \xi) - \mathcal{A}(q)}{\delta} \\ &= \int_0^T \frac{1}{2} \sum_{i=1}^4 \lim_{\delta \rightarrow 0} m_i \frac{\|\dot{q}_i + \delta \dot{\xi}_i\|^2 - \|\dot{q}_i\|^2}{\delta} + \lim_{\delta \rightarrow 0} \frac{U(q + \delta \xi) - U(q)}{\delta} dt \\ &= \int_0^T \left(\sum_{i=1}^4 m_i \langle \dot{q}_i, \dot{\xi}_i \rangle + \sum_{i=1}^4 \left\langle \frac{\partial}{\partial q_i} (U(q(t))), \xi_i \right\rangle \right) dt \\ &= \sum_{i=1}^4 m_i \langle \dot{q}_i, \xi_i \rangle \Big|_{t=0}^{t=T} + \int_0^T \left\langle -m_i \ddot{q}_i + \frac{\partial}{\partial q_i} (U(q(t))), \xi_i \right\rangle dt. \end{aligned}$$

Because the first variation $\delta_\xi \mathcal{A}(q)$ is zero for any ξ , and q satisfies Newton's equation (2), we have

$$(26) \quad \delta_\xi \mathcal{A}(q) = \sum_{i=1}^4 (m_i \langle \dot{q}_i(T), \xi_i(T) \rangle) - \sum_{i=1}^4 (m_i \langle \dot{q}_i(0), \xi_i(0) \rangle) = 0.$$

For $i = 4, 5, 6$, let $\xi^{(i)}(t) \in \mathcal{P}(\mathbf{A}, \mathbf{B})$ satisfy $\xi^{(i)}(0) = 0$ and

$$\xi^{(i)}(T) = \begin{pmatrix} a_4 & a_5 \\ 0 & -a_6 \\ -a_4 & a_5 \\ 0 & \frac{-m_1 a_5 - m_3 a_5 + m_2 a_6}{m_4} \end{pmatrix},$$

where $a_i = 1$, $a_j = 0$ if $j \neq i$. Then from equation (26),

$$\delta_{\xi^{(4)}} \mathcal{A}(q) = (m_1 \dot{q}_{11}(T) - m_3 \dot{q}_{31}(T)) = 0,$$

$$\delta_{\xi^{(5)}} \mathcal{A}(q) = (m_1 \dot{q}_{12}(T) + m_3 \dot{q}_{32}(T) - (m_1 + m_3) \dot{q}_{42}(T)) = 0,$$

$$\delta_{\xi^{(6)}} \mathcal{A}(q) = (-m_2 \dot{q}_{22}(T) + m_2 \dot{q}_{42}(T)) = 0.$$

By the above three equalities and $\sum_{i=1}^4 m_i \dot{q}_{ij}(T) = 0$ for $j = 1, 2$ and $m_1 = m_3, m_2 = m_4$, it is easy to derive that the relation (24) holds.

For $i = 1, 2, 3$, let $\xi^{(i)}(t) \in \mathcal{P}(\mathbf{A}, \mathbf{B})$ satisfy $\xi^{(i)}(T) = 0$ and

$$\xi^{(i)}(0) = \begin{pmatrix} 0 & -a_3 \\ -a_1 & a_2 \\ 0 & \frac{-m_2 a_2 - m_4 a_2 + m_1 a_3}{m_3} \\ a_1 & a_2 \end{pmatrix} R(\theta),$$

where $a_i = 1$, $a_j = 0$ if $j \neq i$. Then

$$\delta_{\xi^{(1)}} \mathcal{A}(q) = -(m_2 \langle \dot{q}_2(0), (-1, 0)R(\theta) \rangle + m_4 \langle \dot{q}_4(0), (1, 0)R(\theta) \rangle) = 0,$$

which is

$$(27) \quad -\dot{q}_{21} \cos(\theta) + \dot{q}_{22} \sin(\theta) + \dot{q}_{41} \cos(\theta) - \dot{q}_{42} \sin(\theta) = 0.$$

$$\delta_{\xi^{(2)}} \mathcal{A}(q) = -(m_2 \langle \dot{q}_2(0), (0, 1)R(\theta) \rangle + (m_2 + m_4) \langle \dot{q}_3(0), (0, -1)R(\theta) \rangle + m_4 \langle \dot{q}_4(0), (0, 1)R(\theta) \rangle) = 0;$$

$$(28) \quad m_2(\dot{q}_{21} \sin(\theta) + \dot{q}_{22} \cos(\theta)) - (m_2 + m_4)(\dot{q}_{31} \sin(\theta) + \dot{q}_{32} \cos(\theta)) + m_4(\dot{q}_{41} \sin(\theta) + \dot{q}_{42} \cos(\theta)) = 0.$$

$$\delta_{\xi^{(3)}} \mathcal{A}(q) = -(m_1 \langle \dot{q}_1(0), (0, -1)R(\theta) \rangle + m_1 \langle \dot{q}_3(0), (0, 1)R(\theta) \rangle) = 0;$$

$$(29) \quad -(\dot{q}_{11} \sin(\theta) + \dot{q}_{12} \cos(\theta)) + (\dot{q}_{31} \sin(\theta) + \dot{q}_{32} \cos(\theta)) = 0.$$

Let

$$A_{i1} = \dot{q}_{i1} - \dot{q}_{i1} \cos(2\theta) + \dot{q}_{i2} \sin(2\theta),$$

$$A_{i2} = \dot{q}_{i2} + \dot{q}_{i1} \sin(2\theta) + \dot{q}_{i2} \cos(2\theta),$$

$$A_{j1} = \dot{q}_{j1} - \dot{q}_{k1} \cos(2\theta) + \dot{q}_{k2} \sin(2\theta),$$

$$A_{j2} = \dot{q}_{j2} + \dot{q}_{k1} \sin(2\theta) + \dot{q}_{k2} \cos(2\theta),$$

for $i = 1, 3$ and $(j, k) = (2, 4)$ or $(j, k) = (4, 2)$. Because $\sum_{i=1}^4 m_i \dot{q}_{ik} = 0$ for $k = 1, 2$, we have

$$(30) \quad m_1 A_{11} + m_2 A_{21} + m_3 A_{31} + m_4 A_{41} = 0, \quad m_1 A_{12} + m_2 A_{22} + m_3 A_{32} + m_4 A_{42} = 0$$

by using the fact $m_1 = m_3$ and $m_2 = m_4$. By using the trigonometric identities $\cos(\theta) = \cos(2\theta)\cos(\theta) + \sin(2\theta)\sin(\theta)$ and $\sin(\theta) = \sin(2\theta)\cos(\theta) - \cos(2\theta)\sin(\theta)$, from equation (27), we have

$$\begin{aligned} & -\dot{q}_{21}\cos(\theta) + \dot{q}_{22}\sin\theta + \dot{q}_{41}(\cos(2\theta)\cos(\theta) + \sin(2\theta)\sin(\theta)) \\ & -\dot{q}_{42}(\sin(2\theta)\cos(\theta) - \cos(2\theta)\sin(\theta)) = 0, \end{aligned}$$

which is

$$(31) \quad -A_{21}\cos(\theta) + A_{22}\sin\theta = 0.$$

Similarly from equation (27), we also have

$$(32) \quad A_{41}\cos(\theta) - A_{42}\sin\theta = 0.$$

From equation (28) and $\sum_{i=1}^4 m_i \dot{q}_{ik} = 0$, we have

$$-m_1(\dot{q}_{11}\sin(\theta) + \dot{q}_{12}\cos\theta) - (m_3 + m_2 + m_4)(\dot{q}_{31}\sin(\theta) + \dot{q}_{32}\cos\theta) = 0.$$

Thanks to equation (29) and above equation, we have

$$(33) \quad \dot{q}_{31}\sin(\theta) + \dot{q}_{32}\cos\theta = 0,$$

$$(34) \quad \dot{q}_{11}\sin(\theta) + \dot{q}_{12}\cos\theta = 0,$$

and

$$(35) \quad (\dot{q}_{21}\sin(\theta) + \dot{q}_{22}\cos\theta) + (\dot{q}_{41}\sin(\theta) + \dot{q}_{42}\cos\theta) = 0.$$

By adding the product of equation (27) and $\sin(\theta)$ to the product of equation (35) and $\cos(\theta)$, the sum is $A_{22} = 0$. Then by equation (31), $A_{21} = 0$. Similarly, we have $A_{41} = A_{42} = 0$. From equation (33),

$$\dot{q}_{31}\sin(\theta) + \dot{q}_{32}\cos\theta + \dot{q}_{31}(\sin(2\theta)\cos(\theta) - \cos(2\theta)\sin(\theta)) + \dot{q}_{32}(\cos(2\theta)\cos(\theta) + \sin(2\theta)\sin(\theta)) = 0,$$

which is

$$(36) \quad A_{31}\sin(\theta) + A_{32}\cos(\theta) = 0.$$

By definition, $A_{31}\sin(2\theta) + A_{32}\cos(2\theta) = (\dot{q}_{31} - \dot{q}_{31}\cos(2\theta) + \dot{q}_{32}\sin(2\theta))\sin(2\theta) + (\dot{q}_{32} + \dot{q}_{31}\sin(2\theta) + \dot{q}_{32}\cos(2\theta))\cos(2\theta)$, which implies $A_{31}\sin(2\theta) + A_{32}\cos(2\theta) = A_{32}$. Hence,

$$(37) \quad A_{31}\cos(\theta) - A_{32}\sin(\theta) = 0.$$

From equations (36) and (37), we have $A_{31} = A_{32} = 0$. Then the equation (30) imply that $A_{kj} = 0$ for $k = 1, 2, 3, 4$ and $j = 1, 2$. Because the relations (25) is equivalent to $A_{kj} = 0$, we complete the proof that $q(t)$ connects very well at $t = 2T$. This also completes the proof of Theorem 1.1.

□

3 Existence of New Solutions

In this section, we prove theorem 1.3 by showing that there exists a minimizing path which is different from the homographic motion for any given $(\theta, \mu) \in \Omega$ in equation (13). We show that the action of the test path $\bar{q}(t)$ with constant velocity for a given SPBC \vec{a} is smaller than the minimum action of the path $q^\circ(t)$ for \vec{a}° which is extended to a homographic motion. Therefore, there exists a minimizer with lower action than the action of homographic solution.

First, the homographic motion can be obtained by extending the corresponding minimizing path $q^\circ(t)$ on $[0, T]$ of a particular SPBC \vec{a}° in Γ . Both the initial and ending configurations $q^\circ(0)$ and $q^\circ(T)$ are rhombus and they satisfy the SPBC. Second, we assume that the test path $\bar{q}(t)$ is formed by connecting the straight line with constant velocity from the starting configuration $Qstart$ to the ending configuration $Qend$ for a given \vec{a} . Both actions $\mathcal{A}(q^\circ(t))$ and $\mathcal{A}(\bar{q}(t))$ on $[0, T]$ are explicit continuous functions of (θ, μ) given by formula (8) and (11) respectively. Although the corresponding actions can be calculated by hand, they are computed by a Matlab program.

3.1 Action of the path which is extended to a homographic solution

The configuration q is called a central configuration if q satisfies the following nonlinear algebraic equation system:

$$(38) \quad \lambda(q_i - c) - \sum_{j=1, j \neq i}^n \frac{m_j(q_i - q_j)}{|q_i - q_j|^3} = 0, \quad 1 \leq i \leq n,$$

for a constant λ , where $c = (\sum m_i q_i)/M$ is the center of mass and $M = m_1 + m_2 + \dots + m_n$ is the total mass. We recall the fact that coplanar central configurations always admit homographic solutions where each body executes a similar Keplerian ellipse of eccentricity e , $0 \leq e \leq 1$. When $e = 0$, the relative equilibrium solutions are consisting of uniform circular motion for each of the masses about the common center of mass. When $e = 1$, the homographic solutions degenerate to a homothetic solution which includes total collision, together with a symmetric segment of ejection. Gordon found that for fixed period \mathcal{T}° , all of the homographic solutions have the same action ([18]). Consider the homographic solution of the four-body problem in rhomboid configuration

$$q_k^\circ(t) = r_k(\cos(\omega t + \rho_k), \sin(\omega t + \rho_k)), k = 1, 2, 3, 4,$$

where $r_k > 0$ is the radius and $\rho_k = \frac{(k-1)\pi}{2} + \alpha_0, k = 1, 2, 3, 4$. ω and α_0 are chosen to make the boundary configurations $q^\circ(0)$ and $q^\circ(T)$ satisfy SPBC. By the results of the central configurations with some equal masses [1, 20, 29], we can assume that $r_1 = r_3$ and $r_2 = r_4$ because $m_1 = m_3$ and $m_2 = m_4$. It is easy to find the following relations by Newtonian equations (2):

$$(39) \quad -\omega^2 + \frac{2m_2}{(r_1^2 + r_2^2)^{3/2}} + \frac{m_1}{4r_1^3} = 0,$$

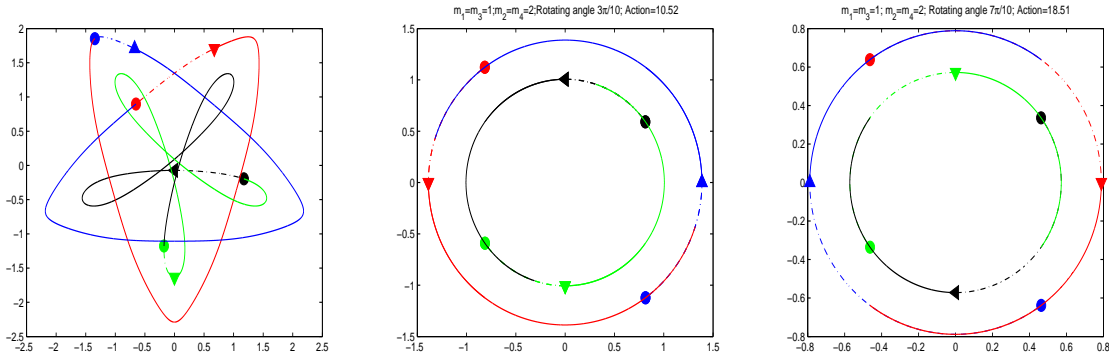


Figure 5: $(\theta, \mu) = (\frac{4\pi}{5}, 2)$. Left: Minimizing path with action 9.748; Middle: Homographic solution $\omega = \frac{3\pi}{10}$ with action 10.52; Right: Homographic solution $\omega = \frac{7\pi}{10}$ with action 18.51.

$$(40) \quad -\omega^2 + \frac{2m_1}{(r_1^2 + r_2^2)^{3/2}} + \frac{m_2}{4r_2^3} = 0.$$

The minimum period is $\mathcal{T}^\circ = \frac{2\pi}{\omega}$. For any given positive ω , m_1 and m_2 , r_1 and r_2 are uniquely determined by the above two equations. The minimum value of the action functional (1) on $[0, T]$ could be computed as

$$\begin{aligned} \mathcal{A}(q^\circ(t)) &= \int_0^T \sum_{k=1}^4 \frac{1}{2} m_k |\dot{q}_k^\circ(t)|^2 + U(q^\circ(t)) dt \\ &= \left(m_1 \omega^2 r_1^2 + m_2 \omega^2 r_2^2 + 4 \frac{m_1 m_2}{\sqrt{r_1^2 + r_2^2}} + \frac{m_1^2}{2r_1} + \frac{m_2^2}{2r_2} \right) T \\ &= 3\omega^2 (m_1 r_1^2 + r_2^2 m_2) T. \end{aligned}$$

For fixed (θ, μ) , there are different central configurations satisfying SPBC to generate homographic solutions. For example, when $\theta = \frac{4\pi}{5}$, $\omega = \frac{\pi}{2} - \frac{\pi}{5} = \frac{3\pi}{10}$ (see middle in Figure 5) or $\omega = \frac{\pi}{2} + \frac{\pi}{5} = \frac{7\pi}{10}$ (see right in Figure 5). But in order to have a minimizing action over the time interval $[0, T]$, the bodies in homographic solutions should rotate an angle as small as possible in $[0, T]$. By the structure of our prescribed boundary conditions, $\omega = |\frac{\pi}{2} - \theta| \frac{1}{T}$ if $0 < \theta < \pi$, or $\omega = |\frac{3\pi}{2} - \theta| \frac{1}{T}$ if $\pi \leq \theta < 2\pi$. So, for a given (θ, μ) , the action of the homographic solution in $(0, T)$ is given by equation (8).

In particular, if $\mu = 1$, i.e. $m_1 = m_2 = 1$, then $r_1 = r_2$ and $r_1^2 = \left(\frac{2\sqrt{2}+1}{4}\omega^{-2}\right)^{2/3}$ by equation (39).

$$(41) \quad \mathcal{A}_\diamond(\theta, 1) = \begin{cases} 6 \left(\frac{2\sqrt{2}+1}{4}\right)^{2/3} (|\frac{\pi}{2} - \theta|)^{2/3} T^{1/3} & \text{if } 0 < \theta < \pi, \\ 6 \left(\frac{2\sqrt{2}+1}{4}\right)^{2/3} (|\frac{3\pi}{2} - \theta|)^{2/3} T^{1/3} & \text{if } \pi \leq \theta < 2\pi. \end{cases}$$

Given any $(\theta, \mu) \in (0, 2\pi) \times \mathbf{R}^+$, let k be a positive parameter such that $k\theta \in (0, 2\pi)$. Let $\varrho = \frac{\omega(k\theta)}{\omega(\theta)}$. By the equations (39) and (40), it is easy to derive

$$(42) \quad \mathcal{A}_\diamond(k\theta, \mu) = \varrho^{\frac{2}{3}} \mathcal{A}_\diamond(\theta, \mu).$$

3.2 Action of a test path

For any fixed SPBC \vec{a}_{test} and $T = 1$, the test path $\bar{q}(t)$ with constant velocity connecting the structural prescribed boundaries $Qstart$ and $Qend$ is given by equation (10). Then the action \mathcal{A}_{Tpath} of the test path is an explicit continuous function of (θ, μ) and it is given by equation (11). To get lower action \mathcal{A}_{Tpath} of a test path, we need to pick up an appropriate SPBC \vec{a}_{test} . It is better to have several SPBC for different values of (θ, μ) . For example, we use the minimizer $\vec{a} = [0.6676542303, 1.11499232, 0.5099504088, 0.6676542314, 1.11499232, 0.5099504078]$ for $\theta = \frac{4}{5}\pi$ and $\mu = 1$ as the fixed SPBC \vec{a}_{test} to estimate the action of the test path for all (θ, μ) . The formula (11) becomes

$$\begin{aligned} \mathcal{A}_{Tpath}(\theta, \mu) = & 0.81184 + 2.48644 \cos(\theta) - 0.80792 \sin(\theta) + 2.4864 \mu^{-1} + 0.81184 \mu + \\ & 2.4864 \cos(\theta) \mu - 0.80792 \sin(\theta) \mu + 2.4864 \mu^2 + \int_0^1 [3.0861 \mu^2 + t(1.3618 \sin(\theta) \mu^2 + \\ & 7.2471 \cos(\theta) \mu - 2.9777 \sin(\theta) \mu + 6.1721 \mu^2 + 2.8578 \cos(\theta) \mu^2) + t^2(2.6985 \mu + \\ & 1.3618 \sin(\theta) \mu^2 + 7.2471 \cos(\theta) \mu - 2.9777 \sin(\theta) \mu + \\ & 3.8979 \mu^2 + 2.8578 \cos(\theta) \mu^2 + 4.9729)]^{-1/2} + \dots dt \end{aligned}$$

Here we only list the kinetic energy and the one term of potential energy. The integrals only involve the form of $\int_0^1 (a + bt + ct^2)^{-1/2} dt$ which can be integrated explicitly by trigonometric substitution.

3.3 The possible region Ω

Here we describe how we do the numerical computations for the region $\Omega_{\vec{a}_{test}}$ on which $\mathcal{A}_\diamond(\theta, \mu) > \mathcal{A}_{Tpath}(\theta, \mu)$. We are going to compute $\mathcal{A}_{Tpath}(\theta, \mu)$ for the fixed SPBC $\vec{a}_{test} = [0.6676542303, 1.11499232, 0.5099504088, 0.6676542314, 1.11499232, 0.5099504078]$ which is a minimizer of $\tilde{\mathcal{A}}$ for $(\theta, \mu) = (\frac{4\pi}{5}, 1)$.

For fixed $\mu = 1$, the graph of $\mathcal{A}_\diamond(\theta, 1)$ can be easily obtained from equation (41) and the graph of $\mathcal{A}_{Tpath}(\theta, 1)$ is given by figure 3. By direct computation, $\mathcal{A}_\diamond(0.78\pi, 1) = 5.3497 > 5.3444 = \mathcal{A}_{Tpath}(0.78\pi, 1)$ but $\mathcal{A}_\diamond(0.77\pi, 1) = 5.2216 < 5.4085 = \mathcal{A}_{Tpath}(0.77\pi, 1)$, and $\mathcal{A}_\diamond(1.11\pi, 1) = 6.6722 > 6.5124 = \mathcal{A}_{Tpath}(1.11\pi, 1)$ but $\mathcal{A}_\diamond(1.12\pi, 1) = 6.5576 < 6.6465 = \mathcal{A}_{Tpath}(1.12\pi, 1)$. So there exist $0.77\pi < \theta_0 < 0.78\pi$ and $1.11\pi < \theta_1 < 1.12\pi$ such that for any $\theta \in (\theta_0, \theta_1)$, $\mathcal{A}_\diamond(\theta, 1) > \mathcal{A}_{Tpath}(\theta, 1)$.

For fixed $\theta = \frac{4\pi}{5}$, we compute $\mathcal{A}_\diamond(\frac{4\pi}{5}, \mu)$ and $\mathcal{A}_{Tpath}(\frac{4\pi}{5}, \mu)$. We find that $\mathcal{A}_\diamond(\frac{4\pi}{5}, \mu) > \mathcal{A}_{Tpath}(\frac{4\pi}{5}, \mu)$ for $\mu_0 < \mu < \mu_1$ where $0.8 < \mu_0 < 0.9$ and $1.2 < \mu_1 < 1.3$ (see figure 6). But the

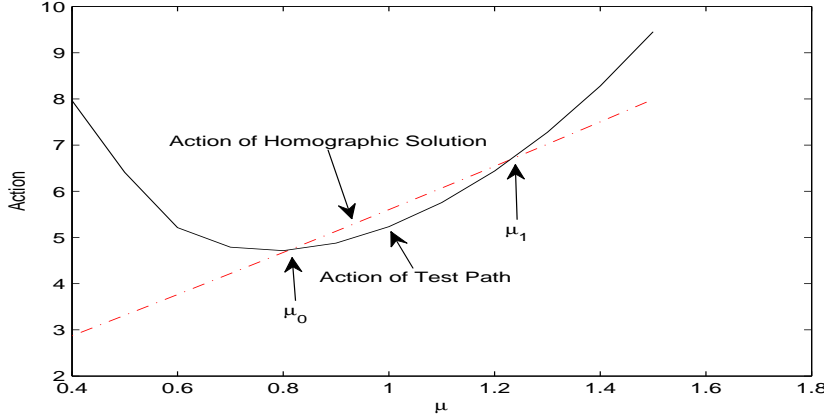


Figure 6: Fixed $\theta = \frac{4\pi}{5}$. Use $\vec{a}_{test} = [0.6676542303, 1.11499232, 0.5099504088, 0.6676542314, 1.11499232, 0.5099504078]$ as fixed SPBC for the test path. Test path has lower action than homographic solution when $\mu_0 < \mu < \mu_1$.

action for the minimizing path is less than the action of homographic solution for larger range of μ . In fact, we can prove that $\mathcal{A}_{\diamond}(\frac{4\pi}{5}, \mu) > \tilde{\mathcal{A}}$ when $0.5 \leq \mu \leq 2.1$.

We fix μ at different value to find the intervals of θ such that $\mathcal{A}_{\diamond}(\theta, \mu) > \mathcal{A}_{Tpath}(\theta, \mu)$. We use $\mathcal{A}_{\diamond}(\frac{4\pi}{5}, \mu)$ to generate $\mathcal{A}_{\diamond}(\theta, \mu)$ by equation (42). For the fixed SPBC \vec{a}_{test} , the region $\Omega_{\vec{a}_{test}}$ is presented in figure 4.

It is easy to know that the action of homographic solution $\mathcal{A}_{\diamond}(\theta, \mu)$ is independent of the choice of SPBC \vec{a}_{test} but the action of test path $\mathcal{A}_{Tpath}(\theta, \mu)$ strongly depends on the choice of SPBC \vec{a}_{test} . The figure 7 shows the different $\Omega_{\vec{a}_{test}}$ when the test pathes are generated from different SPBC \vec{a}_{test} which are the minimizers of $\tilde{\mathcal{A}}$ for same angle $\theta = \frac{4\pi}{5}$ and different mass ratio μ . The SPBC \vec{a}_{test} corresponding to the region $\Omega_{\vec{a}_{test}}$ in figure 7 from top to bottom are (1) $\vec{a}_{test} = [0.8347577868, 0.8492284757, 1.107411045, 0.6740939528, 1.7071110, 0.072136065]$ for $(\theta, \mu) = (\frac{4\pi}{5}, 2)$; (2) $\vec{a}_{test} = [0.6676542303, 1.11499232, 0.5099504088, 0.6676542314, 1.11499232, 0.5099504078]$ for $(\theta, \mu) = (\frac{4\pi}{5}, 1)$; (3) $\vec{a}_{test} = [0.6216336897, 1.197204657, 0.347804861, 0.6658203645, 0.9561601763, 0.6379731628]$ for $(\theta, \mu) = (\frac{4\pi}{5}, 0.8)$; (4) $\vec{a}_{test} = [0.5350313653, 1.354931439, 0.0572523078, 0.6625485, 0.674032487, 0.8789531194]$ for $(\theta, \mu) = (\frac{4\pi}{5}, 0.5)$.

The possible admissible set Ω contains the union of the regions in figure 7 but larger range can be expected by refining the test path.

3.4 Classification of solutions according to (θ, μ)

Now it is ready to prove theorem 1.3 and to classify the minimizing solutions based on the rotation angle θ and mass ratio μ . Since the action of test path is lower than the action of

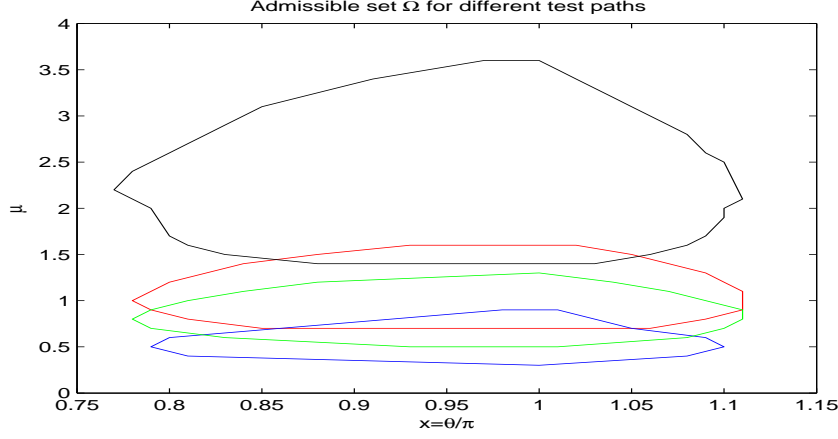


Figure 7: Different sets $\Omega_{\vec{a}_{test}}$ for different test path. The SPBC \vec{a}_{test} from top to bottom are minimizers for same rotation angle $\theta = \frac{4\pi}{5}$ and different mass ratio $\mu = 2, 1, 0.8, 0.5$.

homographic solutions when $(\theta, \mu) \in \Omega$, there exists a minimizer of $\tilde{\mathcal{A}}$ by theorem 2.1 and theorem 1.1. Its corresponding path $q^*(t)$ in $[0, T]$ can be extended to a classical non-collision non-homographic solution of Newtonian equation (2) for time $t \in [0, \infty)$. By the extension formula (7),

$$q(t) = \sigma^k(q(t - 2kT))R(-2k\theta) \text{ for } t \in (2kT, (2k + 2)T] \text{ and } k \in \mathbf{Z}^+,$$

and $\sigma^2 = [1, 2, 3, 4]$, the orbit of the solution is assembled out the sides $q_i(t), t \in [0, 4T]$ by rotation only. For any $(\theta, \mu) \in \Omega$, the non-homographic solution $q(t)$ can be classified as follows.

(1) By the extension formula, it is easy to show that $q(t)$ is a quasi-periodic solution if θ is not commensurable with π by the fact that the rotation matrix $R(-2k\theta)$ can not be an identity matrix for any integer k . Some quasi-periodic solutions are illustrated in figure 8.

(2) If θ is commensurable with π and $\theta = \frac{P}{Q}\pi$ where the positive integers P and Q are relatively prime, then $q(t) = \sigma^{2Q}(q(t - 4QT))R(-4P\pi) = q(t - 4QT)$ which implies that $q(t)$ is a periodic solution. The trajectory sets $\{q_i(t) | t \in (2k, (2k+2)T)\}$ of the given i th-body are all different for $0 \leq k < Q$, since the rotation matrix $R(-2k\frac{P}{Q}\pi)$ is not identity matrix. The four trajectories on which the four body travel in $t \in (0, 2QT)$ are all different. So the minimum period is between $2QT$ and $4QT$.

- When Q is even, then $q(t) = \sigma^Q(q(t - 2QT))R(-2P\pi) = q(t - 2QT)$ because $\sigma^2 = [1, 2, 3, 4]$. So the four different trajectories in $t \in (0, 2QT)$ are closed on their own at $t = 2QT$, i.e. $q(2QT) = q(0)$. $q_i(k_1T) \neq q_j(k_2T)$ if $i \neq j$ and $0 \leq k_1, k_2 \leq Q$, i.e. trajectories of i -th body and j -th body do not meet at the end of any piece orbit. The periodic solution is non-choreographic and the minimum period is $\mathcal{T} = 2QT$. Each closed curve has $\frac{2QT}{4T} = \frac{Q}{2}$ sides. In particular, when $Q = 4$, each closed curve is ellipse-like (two sides); when $Q = 6$, each closed curve is triangle-like (three sides); when $Q = 8$, each closed curve is diamond-like (four sides); and so on. See figure 9.

- When Q is odd, there are four cases.
 $\sigma^Q = \sigma$ and $q(t) = \sigma^Q(q(t - 2QT))R(-2P\pi) = \sigma(q(t - 2QT))$. So $q_1(t + 2QT) = q_3(t)$, $q_3(t + 2QT) = q_1(t)$, and $q_2(t + 2QT) = q_4(t)$, $q_4(t + 2QT) = q_2(t)$, which means that q_1 chases q_3 and q_2 chases q_4 . We have different cases on whether the closed orbit for q_2 and q_4 is the same as the closed orbit for q_1 and q_3 .

Case 1: If $\mu \neq 1$, the ratio between the distance of the center of mass for m_1 and m_3 to the origin and the distance of the center of mass for m_2 and m_4 to origin is μ at both $t = 0$ and $t = T$. By the extension formula (7), bodies q_1 and q_3 rotate around their center of mass, and bodies q_2 and q_4 rotate around their center of mass respectively. They can not have the same orbits. Otherwise the orbit of the center of mass for m_1 and m_3 would be the same as the orbit of the center of mass for m_2 and m_4 since $m_1 = m_3$ and $m_2 = m_4$. This contradicts to the ratio $\mu \neq 1$. Therefore, if $\mu \neq 1$, the periodic solution $q(t; \theta, \mu, \vec{a}_0)$ is a double-choreographic solution. The minimum period is $\mathcal{T} = 4QT$. Each closed curve has Q sides. Body q_1 chases body q_3 on a closed curve and body q_2 chases body q_4 on another closed curve. $q_1(t + 2QT) = q_3(t)$ and $q_3(t + 2QT) = q_1(t)$. $q_4(t + 2QT) = q_2(t)$ and $q_2(t + 2QT) = q_4(t)$. See figure 10.

Case 2: If $\mu = 1$ and P is odd, by the extension formula (7) it is easy to check that the intersection is empty between the sets of $\{q_1(2kT), q_3(2kT) | k \text{ is a nonnegative integer}\}$ and $\{q_2((2k + 1)T), q_4((2k + 1)T) | k \text{ is a nonnegative integer}\}$. So the orbit of q_1 and q_3 can not be the same as the orbit of q_2 and q_4 . The periodic solution $q(t; \theta, \mu, \vec{a}_0)$ is a double-choreographic solution with minimum period $\mathcal{T} = 4QT$. Body q_1 chases body q_3 on a closed curve and body q_2 chases body q_4 on another closed curve. See figure 11.

Case 3: If $\mu = 1$, P is even and the initial configuration $q(0)$ is geometrically same to the ending configuration $q(T)$, i.e. $a_{i0} = a_{(i+3)0}$ for $i = 1, 2, 3$, then the set $\{q_1(kT), q_3(kT)\}$ is equal to the set $\{q_2(kT), q_4(kT)\}$ by the extension formula (7). The orbit of q_1 and q_3 is the same as the orbit of q_2 and q_4 . Then the periodic solution is a choreographic solution. The minimum period is $\mathcal{T} = 4QT$. The closed curve has Q sides.

(A) If $\frac{Q-1}{2}$ is odd, then the four bodies chase each other on the closed curve in the order of q_1, q_2, q_3, q_4 , and then q_1 , i.e. $q_1(t + QT) = q_2(t)$, $q_2(t + QT) = q_3(t)$, $q_3(t + QT) = q_4(t)$, and $q_4(t + QT) = q_1(t)$. See figure 12.

(B) If $\frac{Q-1}{2}$ is even, then the four bodies chase each other on the closed curve in the order of q_1, q_4, q_3, q_2 , and then q_1 , i.e. $q_1(t + QT) = q_4(t)$, $q_4(t + QT) = q_3(t)$, $q_3(t + QT) = q_2(t)$, and $q_2(t + QT) = q_1(t)$. See figure 13.

Case 4: If $\mu = 1$, P is even and the initial configuration $q(0)$ is not geometrically same to the ending configuration $q(T)$, i.e. $(a_{10}, a_{20}, a_{30}) \neq (a_{40}, a_{50}, a_{60})$, then $q_1(k_1T)$ and $q_3(k_1T)$ can not match with $q_2(k_2T)$ and $q_4(k_2T)$ for any nonnegative integer k_1 and k_2 . So the periodic solution is a double choreographic solution. Each closed curve has Q sides. The minimum period is $\mathcal{T} = 4QT$. Body q_1 chases body q_3 on a closed curve and body q_2 chases body q_4 on another closed curve. $q_1(t + 2QT) = q_3(t)$ and

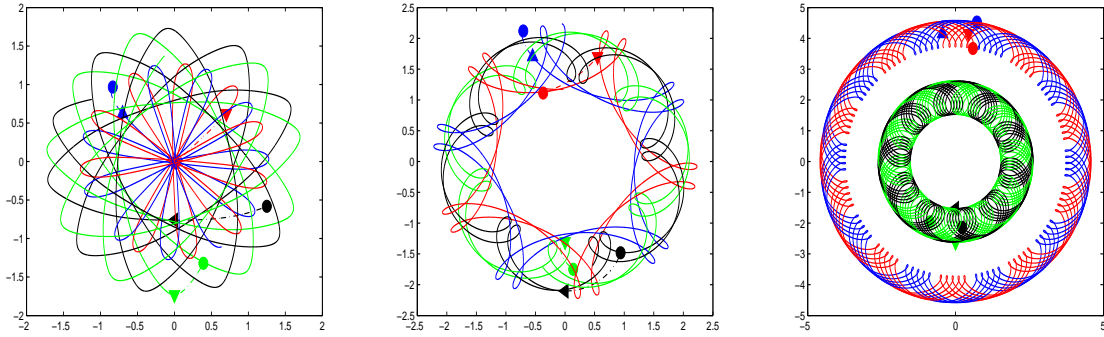


Figure 8: Quasi-Periodic Solutions. From left to right: $(\theta, \mu) = (2.43, 0.5)$ on $[0, 40T]$; $(2.82, 1)$ on $[0, 40T]$; $(3.3, 2)$ on $[0, 220T]$

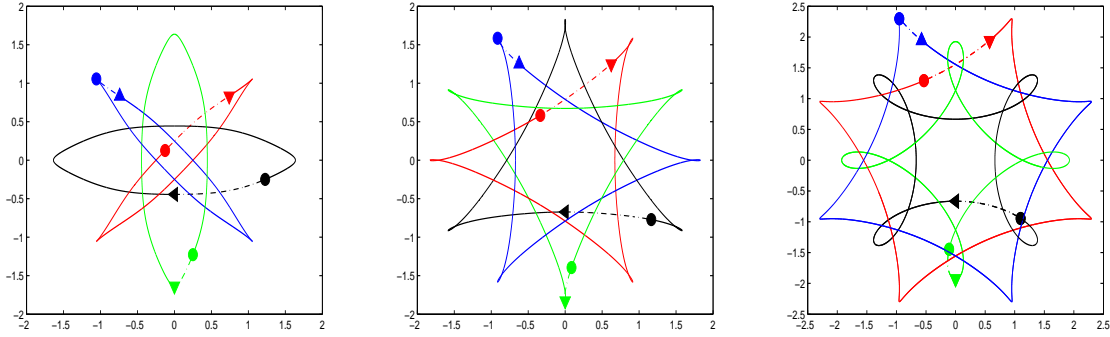


Figure 9: Non-choreographic Periodic Solutions when $\theta = \frac{P}{Q}\pi$ with Q even. From left to right: $(\theta, \mu) = (\frac{3\pi}{4}, 0.8)$; $(\theta, \mu) = (\frac{5\pi}{6}, 1)$; $(\theta, \mu) = (\frac{7\pi}{8}, 1.5)$.

$q_3(t + 2QT) = q_1(t)$. $q_4(t + 2QT) = q_2(t)$ and $q_2(t + 2QT) = q_4(t)$. See figure 14.

4 Linear Stability of the Periodic Solutions

In this section, we provide a rigorous computation to study the linear stability of the periodic solutions. The periodic solutions generated by the local minimizers will be regarded as a \mathcal{T} -periodic solutions to a Hamiltonian system. The linear stability of the periodic solutions will be determined by the eigenvalues of their corresponding monodromy matrix. Suppose that $\gamma(t)$ is a \mathcal{T} -periodic solution to the Hamiltonian system $\dot{\gamma} = J\nabla H(\gamma)$, where $J = \begin{bmatrix} 0 & I \\ -I & 0 \end{bmatrix}$ is the standard symplectic matrix and I is the appropriately sized identity matrix. Let $X(t)$ be the fundamental matrix solution to

$$\dot{\xi} = JD^2H(\gamma(t))\xi, \quad \xi(0) = I.$$

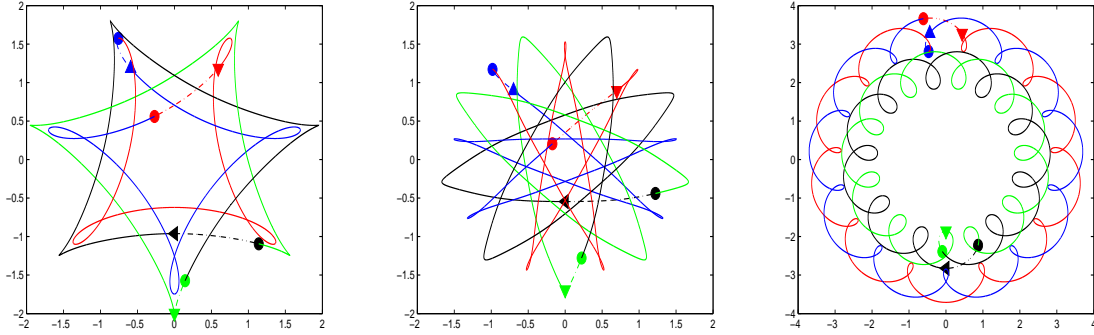


Figure 10: Double Choreographic Solutions when $\mu \neq 1$ and $\theta = \frac{P}{Q}\pi$ with Q odd. From left to right: $(\theta, \mu) = (\frac{6\pi}{7}, 0.8)$; $(\theta, \mu) = (\frac{7\pi}{9}, 0.8)$; $(\theta, \mu) = (\frac{18\pi}{19}, 1.4)$.

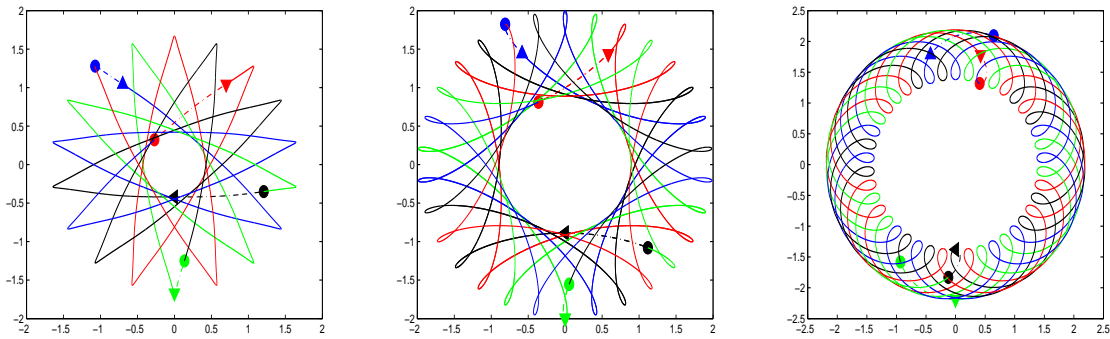


Figure 11: Double Periodic Solutions when $\mu = 1$ and $\theta = \frac{P}{Q}\pi$ with both P and Q odd. From left to right: $(\theta, \mu) = (\frac{7\pi}{9}, 1)$; $(\theta, \mu) = (\frac{13\pi}{15}, 1)$; $(\theta, \mu) = (\frac{23\pi}{21}, 1)$.

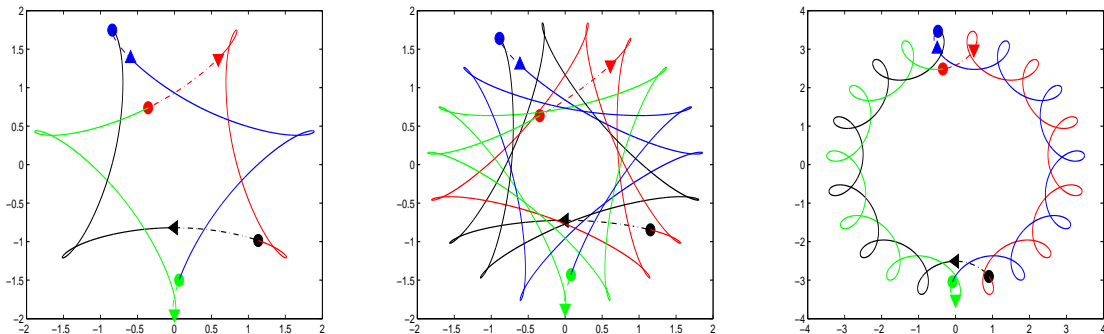


Figure 12: Simple Choreographic Solutions when $\mu = 1$ and $\theta = \frac{P}{Q}\pi$ with P even and $\frac{Q-1}{2}$ odd. Bodies chase each other in the order q_1 (red) \rightarrow q_2 (black) \rightarrow q_3 (blue) \rightarrow q_4 (green) \rightarrow q_1 . From left to right $\theta = \frac{6\pi}{7}$, $\frac{16\pi}{19}$, and $\frac{22\pi}{23}$.

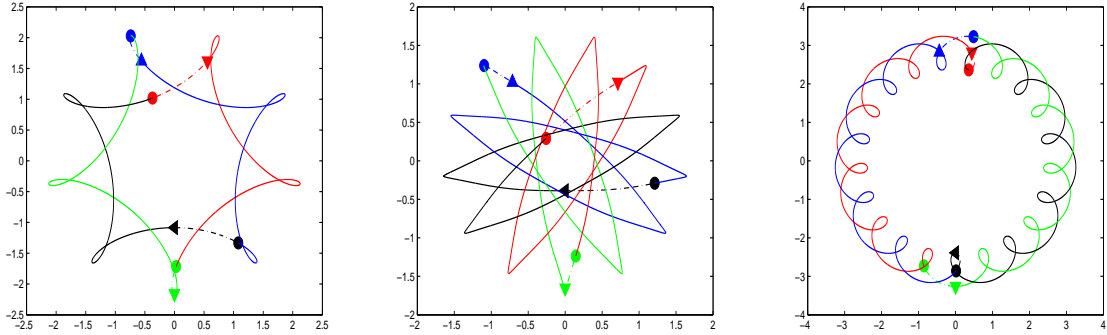


Figure 13: Simple Choreographic Solutions when $\mu = 1$ and $\theta = \frac{P}{Q}\pi$ with P even and $\frac{Q-1}{2}$ even. Bodies chase each other in the order q_1 (red) \rightarrow q_4 (green) \rightarrow q_3 (blue) \rightarrow q_2 (black) \rightarrow q_1 . From left to right $\theta = \frac{8\pi}{9}$, $\frac{10\pi}{13}$, and $\frac{22\pi}{21}$.

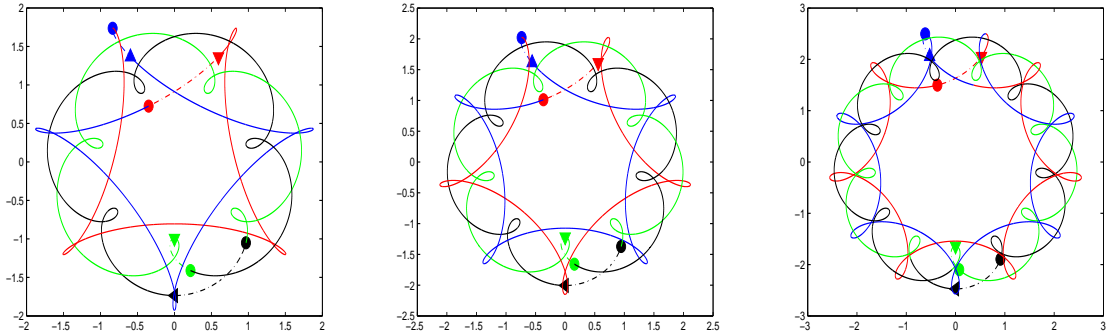


Figure 14: Double Periodic Solutions when $\mu = 1$ and $\theta = \frac{P}{Q}\pi$ with P even and Q odd. From left to right: $(\theta, \mu) = (\frac{6\pi}{7}, 1)$; $(\theta, \mu) = (\frac{8\pi}{9}, 1)$; $(\theta, \mu) = (\frac{12\pi}{13}, 1)$.

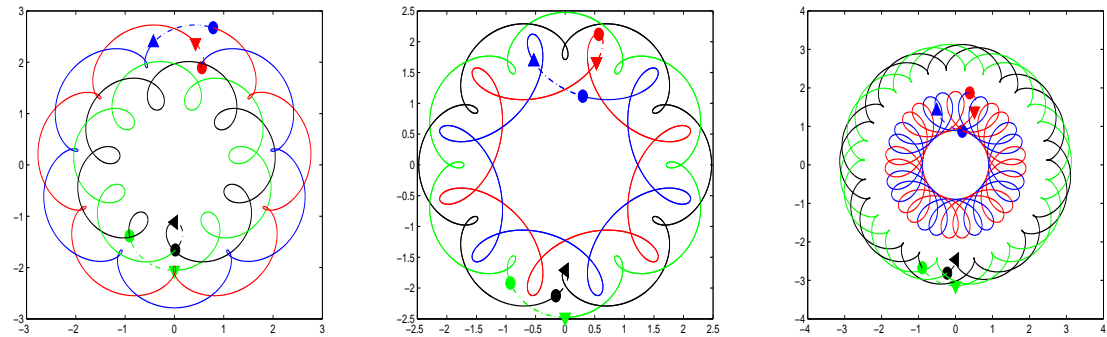


Figure 15: Periodic Solutions for $\theta > \pi$. From left to right $(\theta, \mu) = (\frac{12\pi}{11}, 1.5)$, $(\theta, \mu) = (\frac{13\pi}{12}, 0.8)$, $(\theta, \mu) = (\frac{33\pi}{31}, 0.5)$.

$X(t)$ is symplectic and satisfies $X(t + \mathcal{T}) = X(t)X(\mathcal{T})$ for all t . The matrix $X(\mathcal{T})$ is called the monodromy matrix whose eigenvalues, the characteristic multipliers, determine the linear stability of the periodic solution. Since every integral in the n -body problem yields a multiplier of $+1$, there are eight $+1$ multipliers for a periodic orbit in the planar problem. It is natural to define the linear stability of a periodic solution by examining stability on the reduced quotient space.

Definition 4.1. A periodic solution of the planar n -body problem has eight trivial characteristic multipliers of $+1$. The solution is spectrally stable if the remaining multipliers lie on the unit circle and linearly stable if, in addition, the monodromy matrix $X(\mathcal{T})$ restricted to the reduced space is diagonalizable.

Here we apply standard symplectic transforms to reduce Hamiltonian system to a 10 dimension Hamiltonian system. Such reductions have been constructed in [26] and we include it here for the sake of completeness. The monodromy matrix of the periodic solution $\gamma(t)$ in the reduced system has a pair of $+1$ eigenvalues and the remaining eight eigenvalues must be on the unit circle if the solution is linearly stable.

To eliminate the trivial $+1$ multipliers of a periodic solution, we use Jacobi coordinates and symplectic polar coordinates (see chapter 7 in [23]). Denote $p_i = m_i \dot{q}_i$ as the momentum coordinates and let $\mu_i = \sum_{j=1}^i m_j$ and $M_i = \frac{m_i \mu_{i-1}}{\mu_i}$. Then let

$$\begin{aligned} g_4 &= \frac{m_4 q_4 + m_3 q_3 + m_2 q_2 + m_1 q_1}{m_1 + m_2 + m_3 + m_4}, & G_4 &= p_4 + p_3 + p_2 + p_1; \\ u_2 &= q_2 - q_1, & v_2 &= \frac{\mu_1 p_2}{\mu_2} - \frac{m_2 p_1}{\mu_2}; \\ u_3 &= q_3 - \frac{m_2 q_2 + m_1 q_1}{m_1 + m_2}, & v_3 &= \frac{\mu_2 p_3}{\mu_3} - \frac{m_3 (p_2 + p_1)}{\mu_3}; \\ u_4 &= q_4 - \frac{m_3 q_3 + m_2 q_2 + m_1 q_1}{m_1 + m_2 + m_3}, & v_4 &= \frac{\mu_3 p_4}{\mu_4} - \frac{m_4 (p_3 + p_2 + p_1)}{\mu_4}. \end{aligned}$$

The new Hamiltonian is

$$H_2(u_2, u_3, u_4, v_2, v_3, v_4) = \frac{v_2^2}{2M_2} + \frac{v_3^2}{2M_3} + \frac{v_4^2}{2M_4} - U_2.$$

U_2 is the corresponding potential energy in the new coordinates and similarly U_3, U_4 in the below are the potential energy in the different coordinates. The new Hamiltonian is independent of g_4 and G_4 , the center of mass and total linear momentum respectively. This reduces the dimension by four from 16 to 12.

Next we change to symplectic polar coordinates to eliminate the integrals due to the angular momentum and rotational symmetry. Set

$$\begin{aligned} u_i &= (r_i \cos(\theta_i), r_i \sin(\theta_i)) \\ v_i &= (R_i \cos(\theta_i) - \frac{\Theta_i}{r_i} \sin(\theta_i), R_i \sin(\theta_i) + \frac{\Theta_i}{r_i} \cos(\theta_i)) \end{aligned}$$

for $i = 2, 3, 4$. Then the new Hamiltonian becomes

$$H_3 = \frac{R_2^2 r_2^2 + \Theta_2^2}{2M_2 r_2^2} + \frac{R_3^2 r_3^2 + \Theta_3^2}{2M_3 r_3^2} + \frac{R_4^2 r_4^2 + \Theta_4^2}{2M_4 r_4^2} - U_3.$$

Note that the Hamiltonian H_3 has only terms of difference angles. This suggests making a final symplectic change of coordinates by leaving the radial variables alone. Use the generating function $S = \Theta_2 x_2 + \Theta_3 (x_3 + x_2) + \Theta_4 (x_4 + x_3 + x_2)$, and so

$$\theta_2 = x_2, \theta_3 = x_3 + x_2, \theta_4 = x_4 + x_3 + x_2;$$

$$\Theta_2 = X_2 - X_3, \Theta_3 = X_3 - X_4; \Theta_4 = X_4.$$

The new Hamiltonian will be independent of x_2 which means that $X_2 = \Theta_2 + \Theta_3 + \Theta_4$ (total angular momentum) is an integral, and x_2 is an ignorable variable. Setting $X_2 = c$ and plugging into the Hamiltonian H_3 yields

$$H_4 = \frac{R_2^2 r_2^2 + (c - X_3)^2}{2M_2 r_2^2} + \frac{R_3^2 r_3^2 + (X_3 - X_4)^2}{2M_3 r_3^2} + \frac{R_4^2 r_4^2 + X_4^2}{2M_4 r_4^2} - U_4.$$

This reduces the system to 10 dimensions, with the variables $z = (r_2, r_3, r_4, x_3, x_4, R_2, R_3, R_4, X_3, X_4)$.

Because H_4 is a Hamiltonian system, the monodromy matrix $X(\mathcal{T})$ is symplectic. Its periodic solution $\gamma(t)$ will generate an eigenvector of $X(\mathcal{T})$. In fact, $\gamma(t)$ is a solution of $\dot{z} = J\nabla H_4(z)$ with initial condition $z(0) = \gamma(0)$. Then $\dot{\gamma}(t) = JD^2 H_4(\gamma(t))\dot{\gamma}(t)$. This implies that $\dot{\gamma}(t)$ satisfies the associated linear system

$$\dot{\xi} = JD^2 H_4(\gamma(t))\xi, \quad \xi(0) = \dot{\gamma}(0).$$

Since $X(t)$ is the fundamental solution of the above linear system, $\dot{\gamma}(t) = X(t)\dot{\gamma}(0)$, which implies $X(\mathcal{T})\dot{\gamma}(0) = \dot{\gamma}(\mathcal{T}) = \dot{\gamma}(0)$. Because $X(\mathcal{T})$ is symplectic, $J^{-1}X(\mathcal{T})J = X(\mathcal{T})$. Then $X(\mathcal{T})J\dot{\gamma}(0) = J\dot{\gamma}(0)$. So the Monodromy matrix has two +1 multipliers, leaving the remaining eight eigenvalues to determine the linear stability of the periodic solution. Because the eigenvalues of a symplectic matrix occur in quadruples $(\lambda, \lambda^{-1}, \bar{\lambda}, \bar{\lambda}^{-1})$, we have the following lemma.

Lemma 4.2. *Let X be a symplectic matrix and $W = \frac{1}{2}(X + X^{-1})$. Then the eigenvalues of X are all on the unit circle if and only if all of the eigenvalues of W are real and in $[-1, 1]$.*

Proof. The lemma and its proof are similar to Lemma 4.1 in Roberts' paper [25]. We prove it here for the sake of completeness. Suppose that \vec{v} is an eigenvector of the symplectic matrix X with eigenvalue λ , i.e. $X\vec{v} = \lambda\vec{v}$. Then $X^{-1}\vec{v} = \lambda^{-1}\vec{v}$. $W\vec{v} = \frac{1}{2}(X + X^{-1})\vec{v} = \frac{1}{2}(\lambda + \lambda^{-1})\vec{v}$ from which it follows that $\frac{1}{2}(\lambda + \lambda^{-1})$ is an eigenvalue of W . The map $f : \mathcal{C} \mapsto \mathcal{C}$ given by $f(\lambda) = \frac{1}{2}(\lambda + \lambda^{-1})$ takes the unit circle onto the real interval $[-1, 1]$ while mapping the exterior of the unit disk homeomorphically onto $\mathcal{C} \setminus [-1, 1]$. The lemma follows this assertion immediately. \square

Because the eigenvalue pairs λ and λ^{-1} of X are mapped to the same eigenvalue $\frac{1}{2}(\lambda + \lambda^{-1})$ of W , the multiplicity of eigenvalues of W must be at least two. The two +1 multipliers is still mapped to +1 with multiplicity two. The remaining eight non-one eigenvalues on the unit circle of X for linear stable periodic solution have been mapped to four pairs of real eigenvalues in $(-1, 1)$.

Numerically, a MATLAB program was written using a Runge-Kutta-Fehlberg method with local truncation error of order four to compute the monodromy matrix $X(\mathcal{T})$ of the reduced linearized Hamiltonian H_4 for a periodic solution of planar 4-body problem. Then we compute $W = \frac{1}{2}(X + X^{-1})$ and its eigenvalues. In order to conclude the stability, we first need to improve the estimates of our SPBC \vec{a}_0 and initial conditions of a periodic solutions. There are two steps in searching a solution satisfying SPBC. The first step is to find a solution for a fixed boundary and the second step is to vary the boundary to find a minimizer. In this way, we can easily get a good approximation of the initial conditions of the star pentagon and other solutions with an absolute error tolerance of 10^{-12} . To check whether the global error is within the expected accuracy, we also compute the monodromy matrix and its eigenvalues with several different step sizes for each case as in [26]. By our computation, the four pairs of eigenvalues are all real and distinct in $(-1, 1)$. Returning to the full monodromy matrix, the corresponding eigenvalues are distinct and on the unit circle. Therefore, the corresponding periodic solutions are all linearly stable.

Here we only list the initial conditions for some stable orbits with different rotation angle θ and mass ratio μ in theorem 1.3.

(1) $(\theta, \mu) = (\frac{4\pi}{5}, 1)$, $\mathcal{T} = 20$.

$$q_1(0) = [-0.2997475302, 0.4125670813], \dot{q}_1(0) = [1.114760563, 0.8099231855];$$

$$q_2(0) = [1.195555973, -0.5096218631], \dot{q}_2(0) = [-0.8600513847, -0.003559696213];$$

$$q_3(0) = [-1.011040523, 1.391577897], \dot{q}_3(0) = [0.01444607736, 0.01049661818];$$

$$q_4(0) = [0.1152320804, -1.294523115], \dot{q}_4(0) = [-0.2691552559, -0.8168601074].$$

(2) $(\theta, \mu) = (\frac{4\pi}{5}, 0.5)$, $\mathcal{T} = 20$.

$$q_1(0) = [-0.03365216432, 0.04631823056], \dot{q}_1(0) = [0.8791868243, 0.6387681838];$$

$$q_2(0) = [1.229294751, -0.7817016926], \dot{q}_2(0) = [-0.904358996, -0.2059939437];$$

$$q_3(0) = [-0.762779971, 1.049876561], \dot{q}_3(0) = [-0.1893205096, -0.1375492335];$$

$$q_4(0) = [0.3635695192, -1.410687891], \dot{q}_4(0) = [-0.4753736332, -0.7964439574].$$

(3) $(\theta, \mu) = (\frac{4\pi}{5}, 1.5)$, $\mathcal{T} = 20$.

$$q_1(0) = [-0.4954623785, 0.6819454601], \dot{q}_1(0) = [1.286530639, 0.93472253];$$

$$q_2(0) = [1.17942819, -0.3292799005], \dot{q}_2(0) = [-0.8390962366, 0.1359441271];$$

$$q_3(0) = [-1.196730568, 1.647158317], \dot{q}_3(0) = [0.1671195441, 0.121421328];$$

$$q_4(0) = [-0.05129955936, -1.223455951], \dot{q}_4(0) = [-0.1300038857, -0.8400400324].$$

(4) $(\theta, \mu) = (\frac{7\pi}{8}, 1)$, $\mathcal{T} = 16$.

$$q_1(0) = [-0.3657149699, 0.8829140403], \dot{q}_1(0) = [1.186543081, 0.4914819077];$$

$$q_2(0) = [1.104628492, -1.169044107], \dot{q}_2(0) = [-0.7831641034, 0.3494036031];$$

$$q_3(0) = [-0.7844622398, 1.893859379], \dot{q}_3(0) = [-0.09666570501, -0.04003861407];$$

$$q_4(0) = [0.04554871816, -1.607729312], \dot{q}_4(0) = [-0.3067132724, -0.8008468968].$$

$$(5) (\theta, \mu) = \left(\frac{7\pi}{8}, 1.5\right), \mathcal{T} = 16.$$

$$q_1(0) = [-0.5350773026, 1.291790881], \dot{q}_1(0) = [1.350250694, 0.5592959079];$$

$$q_2(0) = [1.099754106, -0.9458393211], \dot{q}_2(0) = [-0.7454903418, 0.4733604227];$$

$$q_3(0) = [-0.9513025743, 2.296647577], \dot{q}_3(0) = [0.05662296548, 0.02345549633];$$

$$q_4(0) = [-0.1088341884, -1.446452984], \dot{q}_4(0) = [-0.1924254315, -0.8618613589].$$

$$(6) (\theta, \mu) = \left(\frac{7\pi}{9}, 1\right), \mathcal{T} = 36.$$

$$q_1(0) = [-0.27004813, 0.3218308291], \dot{q}_1(0) = [1.071180019, 0.8988296083];$$

$$q_2(0) = [1.207641964, -0.3501521227], \dot{q}_2(0) = [-0.8488458756, -0.1158622427];$$

$$q_3(0) = [-1.072721533, 1.278419741], \dot{q}_3(0) = [0.03916771092, 0.03286635046];$$

$$q_4(0) = [0.1351276988, -1.250098447], \dot{q}_4(0) = [-0.2615018538, -0.815833716].$$

Remark 4.3. Without the symplectic reduction, the original Hamiltonian system of the planar four-body problem has 16 dimension. To check the stability of a periodic solution, one can directly compute the eigenvalues of its Monodromy matrix. Thanks a Matlab Program by Professor Robert Vanderbei, the largest absolute values of the eigenvalues for above examples are all 1.0000.

5 Other solutions from different SPBC in the planar 4-body problem

We decide to close our paper by presenting a different SPBC in the planar 4-body problem. They produce some interesting orbits including triple-choreographic solutions where orbits consist of three closed curves. The configurations formed by four-body with some symmetries can be isosceles triangle with one on the axis of symmetry of the triangle, rectangle, square, diamond, kite, and collinear. We numerically found lots of periodic solutions by the different combinations of these symmetrical configurations. Some of known planar 4-body periodic orbits can be found by this method.

Example 5.1. The SPBC is given by two appropriate configuration subspaces $\mathbf{A} \subset (\mathbf{R}^2)^4$ and $\mathbf{B} \subset (\mathbf{R}^2)^4$ as follows.

$$\mathbf{A} = \left\{ \left(\begin{array}{c} 0 \\ 0 \\ 0 \\ 0 \end{array} \begin{array}{c} a_1 \\ a_1 - |a_2| \\ a_1 - |a_2| - |a_3| \\ \frac{-(m_1 a_1 + m_2(a_1 - |a_2|) + m_3(a_1 - |a_2| - |a_3|))}{m_4} \end{array} \right) \in (\mathbf{R}^2)^4 \mid (a_1, a_2, a_3) \in \mathbf{R}^3 \right\},$$

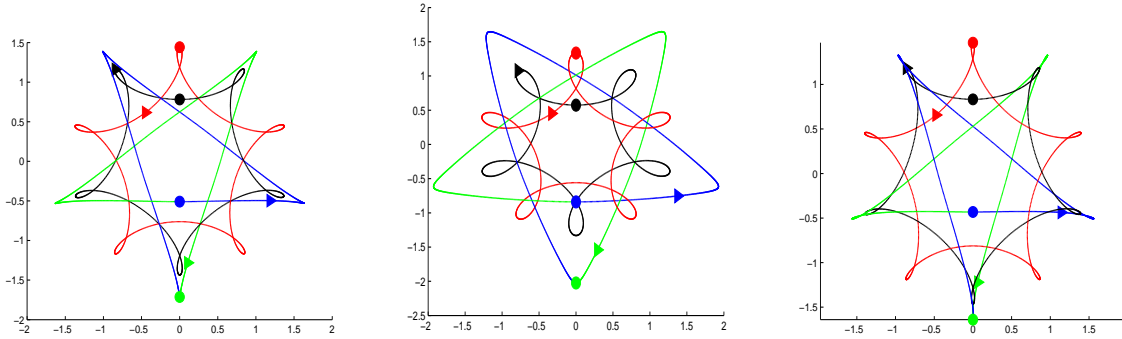


Figure 16: Triple-choreographic Periodic Solutions for $\theta = \frac{4\pi}{5}$ with different masses in Example 5.1.

and

$$\mathbf{B} = \left\{ \left(\begin{array}{cc} 0 & -a_6 \\ 0 & (-m_3a_5 - m_4a_5 + m_1a_6)/m_2 \\ -a_4 & a_5 \\ m_3a_4/m_4 & a_5 \end{array} \right) R(\theta) \in (\mathbf{R}^2)^4 \mid (a_4, a_5, a_6) \in \mathbf{R}^3 \right\}.$$

Geometrically, four bodies start from a collinear configuration $q(0) \in \mathbf{A}$ (circular spots in figures) and end at a triangle configuration $q(T) \in \mathbf{B}$ (triangular spots in figures).

(1) $\theta = \frac{4\pi}{5}$, $m_1 = m_2 = m_3 = m_4 = 1$ (see left graph in Figure 16).

$$q_1(0) = [0, 1.4415], \dot{q}_1(0) = [0.1842, 0]; q_2(0) = [0, 0.7814], \dot{q}_2(0) = [-1.6060, 0];$$

$$q_3(0) = [0, -0.5094], \dot{q}_3(0) = [1.4062, 0]; q_4(0) = [0, -1.7134], \dot{q}_4(0) = [0.0156, 0].$$

(2) $\theta = \frac{4\pi}{5}$, $m_1 = m_2 = 1.5, m_3 = m_4 = 1$ (see middle graph in Figure 16).

$$q_1(0) = [0, 1.3354], \dot{q}_1(0) = [0.4047, 0]; q_2(0) = [0, 0.5743], \dot{q}_2(0) = [-1.6241, 0];$$

$$q_3(0) = [0, -0.8395], \dot{q}_3(0) = [1.6258, 0]; q_4(0) = [0, -2.0250], \dot{q}_4(0) = [0.2033, 0].$$

(3) $\theta = \frac{4\pi}{5}$, $m_1 = m_2 = 0.9, m_3 = m_4 = 1$ (see right graph in Figure 16).

$$q_1(0) = [0, 1.4691], \dot{q}_1(0) = [0.1300, 0]; q_2(0) = [0, 0.8331], \dot{q}_2(0) = [-1.6031, 0];$$

$$q_3(0) = [0, -0.4315], \dot{q}_3(0) = [1.3541, 0]; q_4(0) = [0, -1.6405], \dot{q}_4(0) = [-0.0283, 0].$$

Acknowledgements. This work was partially supported by a grant from the Simons Foundation (#278445 to Zhifu Xie).

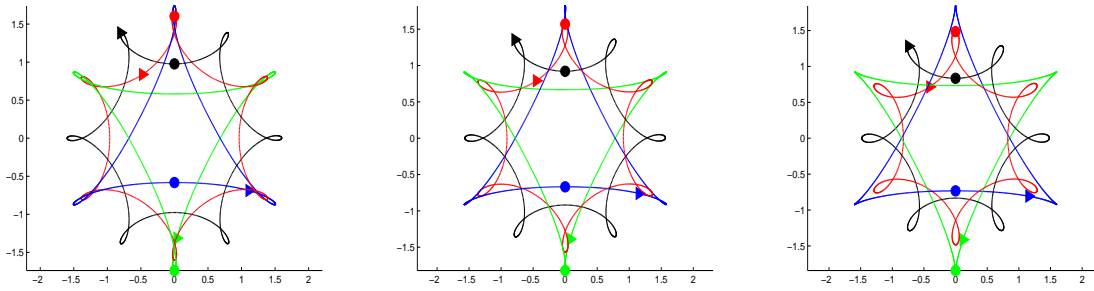


Figure 17: Non-choreographic Periodic Solutions for $\theta = \frac{5\pi}{6}$ with different masses in Example 5.1.

References

- [1] Albouy, Alain; Fu, Yanning; Sun, Shanzhong, Symmetry of Planar Four-Body Convex Central Configurations. *Proc. Royal Soc. A*, **464** (2008), 1355–1365.
- [2] G. Arioli, V. Barutello, S. Terracini, A new branch of Mountain Pass solutions for the choreographical 3-body problem. *Comm. Math. Phys.* 268 (2006), no. 2, 439-463.
- [3] V. Barutello, S. Terracini, Double choreographical solutions for n-body type problems, *Celestial Mechanics and Dynamical Astronomy* (2006) 95:67-80.
- [4] V. Barutello, S. Terracini, Action minimizing orbits in the n-body problem with simple choreography constraint. *Nonlinearity* 17 (2004), no. 6, 2015-2039.
- [5] E. Barrabs, J. Cors, C. Pinyol, J. Soler, Hip-hop solutions of the 2N-body problem. *Celestial Mech. Dynam. Astronom.* 95 (2006), no. 1–4, 55-66.
- [6] R. Broucke, Classification of Periodic Orbits in the Four- and Five-Body Problems, *Ann. N.Y. Acad. Sci.* 1017: 408421 (2004).
- [7] A. Chenciner, Action minimizing solutions in the Newtonian n-body problem: from homology to symmetry. *Proceedings of the International Congress of Mathematicians (Beijing, 2002)*. Higher Ed. Press, Beijing, 279-294, 2002. Erratum. *Proceedings of the International Congress of Mathematicians (Beijing, 2002)*. Higher Ed. Press, Beijing, 651-653, 2002.
- [8] A. Chenciner, R. Montgomery, A remarkable periodic solution of the three body problem in the case of equal masses. *Ann. Math.* 152, 881-901 (2000).
- [9] A. Chenciner, J. Gerver, R. Montgomery, C. Simó, Simple choreographic motions of N bodies: a preliminary study. *Geometry, mechanics, and dynamics*, 287-308, Springer, New York, 2002.
- [10] A. Chenciner, A. Venturelli, Minima of the action integral of the Newtonian problem of four bodies of equal mass in R^3 : "hip-hop" orbits, *Celestial Mech. Dynam. Astronom.* 77 (2000), no. 2, 139-152.

- [11] K. Chen, Existence and minimizing properties of retrograde orbits to the three-body problem with various choices of masses. *Ann. of Math.* (2) 167 (2008), no. 2, 325-348.
- [12] K. Chen, Variational methods on periodic and quasi-periodic solutions for the N-body problem. *Ergodic Theory Dynam. Systems* 23 (2003), no. 6, 1691-1715.
- [13] K. Chen, Removing Collision Singularities from Action Minimizers for the N-Body Problem with Free Boundaries, *Arch. Rational Mech. Anal.* 181 (2006) 311331.
- [14] K. Chen, T. Ouyang, Z. Xia, Action-minimizing periodic and quasi-periodic solutions in the N -body problem, *Math. Res. Lett.* 19 (2012), no. 2, 483-497.
- [15] C. Deng, S. Zhang, Q. Zhou, Rose solutions with three petals for planar 4-body problems, *Sci. China Math*, 2010, 53(12): 3085-3094
- [16] G. Fusco, G.F. Gronchi, P. Negrini, Platonic polyhedra, topological constraints and periodic solutions of the classical N-body problem, *Invent. math.* (2011) 185:283-332.
- [17] D. Ferrario, S. Terracini, On the existence of collisionless equivariant minimizers for the classical n-body problem, *Invent. math.* 155, 305-362 (2004).
- [18] W. Gordon, A minimizing property of Keplerian orbits, *American Journal of Mathematics* 99, no. 5, (1977) 961-971.
- [19] T. Kapela, C. Simó, Computer assisted proofs for nonsymmetric planar choreographies and for stability of the Eight, *Nonlinearity* (2007), **20**, 1241–1255.
- [20] Y. Long and S. Sun, Four-body central configurations with some equal masses. *Arch. Ration. Mech. Anal.* **162** (2002), no. 1, 25–44.
- [21] Dana Mackenzie, TRIPLE STAR SYSTEMS MAY DO CRAZY EIGHTS, *Science* 17 March 2000: Vol. 287 no. 5460 pp. 1910-1912.
- [22] C. Marchal, How the method of minimization of action avoids singularities, *Celestial Mechanics and Dynamical Astronomy*, 83 (2002) 325–353.
- [23] K. Meyer, G. Hall, D. Offin, *Introduction to Hamiltonian Dynamical Systems and the N-Body Problem*, second edition, Springer, 2009.
- [24] C. Moore, Braids in Classical Gravity, *Physical Review Letters* 70 (1993) 3675–3679.
- [25] G. Roberts, Linear stability analysis of the figure-eight orbit in the three-body problem, *Ergod. Th. and Dynam. Sys.* (2007), 27, 1947–1963.
- [26] T. Ouyang, Z. Xie, A new variational method with SPBC and many stable choreographic solutions of the Newtonian 4-body problem, submitted (Available at <http://arxiv.org/pdf/1306.0119.pdf>).
- [27] D. Saari, The manifold structure for collision and for hyperbolic-parabolic orbits in the n-body problem, *J. Differential Equations*, 55 (1984), 300-329.

- [28] Planetary ballet. *Science* 294 (2001) Dec. 14, 2255.
- [29] J. Shi, Z. Xie, Classification of four-body central configurations with three equal masses, *Journal of Mathematical Analysis and Applications* 363 (2010) pp512–524.
- [30] C. Simó, New families of solutions in the N -body problems, Proceedings of the third European Congress of Mathematics, Casacuberta et al. edits, *Progress in Mathematics* (2001), 201, 101–115.
- [31] H.J. Sperling, On the real singularities of the N -body problem, *J. Reine Angew. Math.* 245, (1970), 15–40.
- [32] K.F. Sundman, Mémoire sur le problèdes trois corps. *Acta Math.* 36, (1913), 105–179.
- [33] S. Terracini, On the variational approach to the periodic n -body problem, *Cel. Mech. Dyn. Ast.* 95, 1–4, (2006), 3–25.
- [34] S. Terracini, A. Venturelli, Symmetric trajectories for the $2N$ -body problem with equal masses, *Arch. Rational Mech. Anal.* 184, 465–493 (2007).
- [35] R.J. Vanderbei, New Orbits for the n -Body Problem. In Proceedings of the Conference on New Trends in Astrodynamics, 2003.